JSDSES. **Volume 4**, Issue 2, pp. 90-141 (September, 2025)

Journal of Sustainable Development in Social and Environmental Sciences

Journal Homepage: **https://jsdses.journals.ekb.eg/**

P-ISSN: 2812-6335 E-ISSN: 2812-6343

Spatial Analysis of Hydrological Characteristics and Their Impact on the Stability of the Nile River Banks in the Area Extending from Matai to Al-Fashn

Islam Salama Mohamed Mostafa[1,*], Saber Amin Said Desouki[1]

[1] Department of Geography, Faculty of Arts, Benha University, Egypt.
[*] Corresponding author. *Email address:* islams.salama1977@gmail.com

doi 10.21608/JSDSES.2025.412383.1052

ARTICLE HISTORY
Received: 9-8-2025
Accepted: 11-9-2025
Published: 27-9-2025

KEYWORDS
Hydrological characteristics
River bank stability
Hydro-mechanical properties of soil
River bank soils
Soil hazard classification

ABSTRACT

This study investigates the spatial analysis of hydrological characteristics and their influence on the stability of the Nile River banks in the reach between Matai and Al-Fashn. An integrated analytical framework was adopted, beginning with a long-term assessment of channel dynamics and morphological changes over the past seven decades. Remote sensing and Geographic Information Systems (GIS) techniques were employed to monitor these transformations with high precision, enabling the detection of temporal and spatial changes in channel development, meander evolution, island shifts, and variations in water surface area. Such changes are interpreted as direct responses to hydrological, structural, and climatic drivers and are considered early indicators of bank instability. The findings revealed that hydrological parameters—including discharge, flow velocity, water levels, and suspended sediment load—represent critical determinants of riverbank risk, particularly when combined with soil properties. Hydro-mechanical analysis demonstrated that the complex interaction between hydrological conditions and soil strength parameters is the key factor governing bank stability and the likelihood of erosion or collapse. A spatial risk classification was produced, reflecting varying levels of vulnerability along the banks based on soil–water–depth interactions. The study concludes by recommending an integrated approach to riverbank monitoring and protection that relies on updated spatial data, strict regulatory frameworks, and active community engagement to ensure sustainable management of the Nile corridor.

1. Introduction

Rivers are among the most significant agents of erosion shaping the Earth's surface topography, particularly when compared to wind action in arid regions and glacial activity in polar environments. The continuous flow of water within river channels plays a crucial role in transforming the landscape through processes of erosion, transportation, and deposition. These

fluvial processes often give rise to natural hazards that threaten development efforts. Among these, bank erosion and collapse are recurrent natural phenomena, occurring as a response to the hydrodynamic imbalances within the river system. These processes result from both natural and anthropogenic factors affecting river banks in fluvial systems (Davis & Harden, 2014)

The stability of river banks has become a major concern for the state, particularly following the construction of the High Dam, which triggered significant hydrological changes. These changes have profoundly altered the characteristics of the Nile's River channel in terms of its location, morphology, and the lateral migration of the river path under the influence of hydraulic forces acting on both the river bed and banks. The risks are especially pronounced within meander zones, where imbalances in erosional energy lead to sharp morphological transformations—including the shifting and reshaping of banks, as well as the emergence or disappearance of islands. Such processes result in severe economic losses for residents, particularly in densely populated areas with ongoing economic activity. Bank erosion and collapse also inflict considerable damage on both public and private properties, infrastructure, and natural habitats.

The degree of bank stability along the Nile River is influenced by multiple factors—hydrological, natural, and human-induced. However, hydrological factors are regarded as the most critical, due to their direct relation to the dynamics of river flow and current velocity. These effects have intensified following the construction of the High Dam, which significantly altered the river's hydrological regime—particularly in terms of flow fluctuations, reduced suspended sediment load, and variable flow velocities depending on discharge volumes. These transformations have disrupted the natural balance between erosion and deposition, increasing the susceptibility of river banks to erosion and collapse, in comparison to the impact of other natural and human factors.

2. Study Area

The study area is located along the Nile River channel, extending between Matai in the south and Al-Fashn in the north. This section of the river lies between latitudes 28°22′ and 28°50′30″ N. The total length of the river within this segment is approximately 69.74 km, with an average width of about 1,230 m.

The area is bordered on both the eastern and western sides by the alluvial floodplain, while the eastern limestone plateau approaches the river in some locations, directly overlooking it, and recedes from it in others (Figure 1).

3. Sources of the Study

The current study relied on the following sources:

3.1. Maps

A set of multi-scale maps were utilized, including:

- Topographic maps 1:25,000, edition 1953, issued by the Egyptian Survey Authority; a total of five maps.
- Topographic maps 1:50,000, edition 1991, issued by the General Authority for Survey of Egypt; a total of three maps.
- Hydro-topographic maps of the Nile River bed 1:5,000, issued by the Water Research Center and the Nile Research Institute, editions 1980, 2003, and 2007.
- Geological map 1:500,000, edition 1987, issued by the Egyptian General Petroleum Corporation, produced by Conoco Coral, Sheet NH 36 SW – Beni Suef.
- Landsat TM satellite imagery for the years 2002 and 2023, with a spatial resolution of 30 meters, issued by the U.S. Geological Survey (USGS).

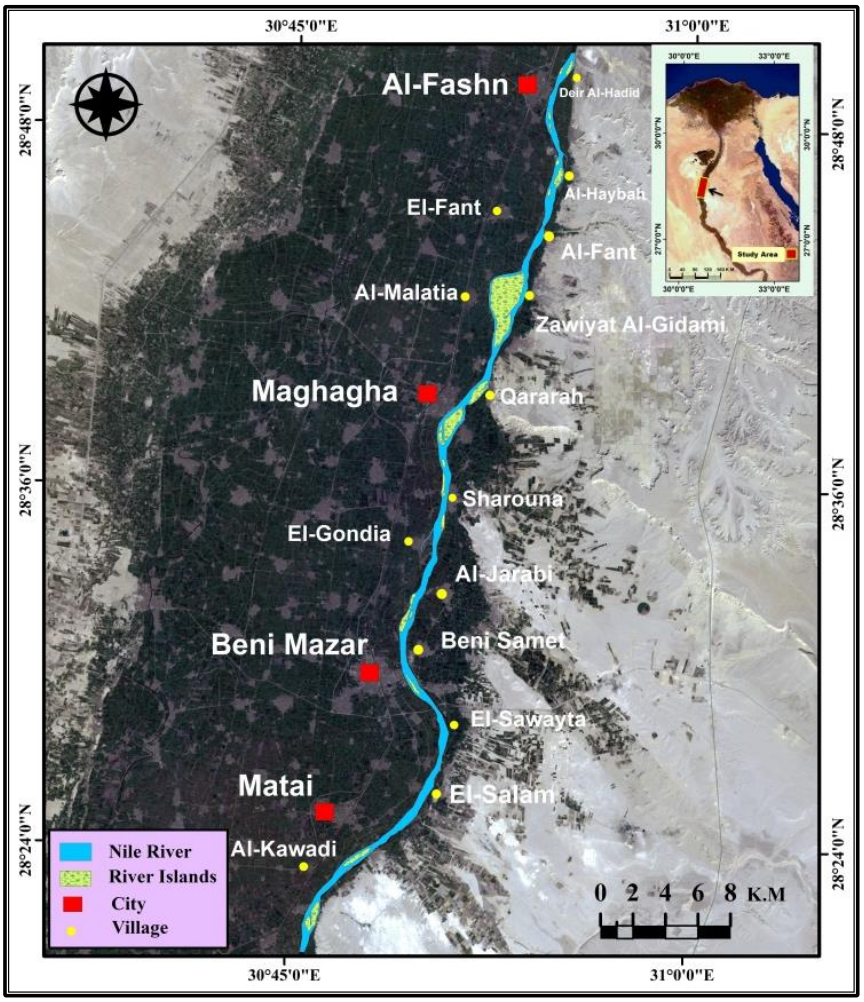

Source: Landsat 8 TM satellite scene, 2023. U.S. Geological Survey (USGS).

Figure 1. Location of the Study Area.

3.2. Field Study

The current study seeks to achieve the following objectives:

It relied primarily on fieldwork as the main source of data collection. This involved conducting direct morphometric measurements of the river banks, observing associated geomorphological features, collecting soil samples from the banks for physical property analysis, recording detailed field observations, and capturing photographic documentation to support the study's findings.

3.3. Literature Review

Although river banks have received considerable attention in various geomorphological studies, most of these investigations have focused on bank erosion and collapse processes, without providing a detailed analysis of the factors influencing bank stability. This highlights a research gap that requires more in-depth and specialized analytical studies aimed at understanding the precise geomorphological mechanisms governing river bank dynamics.

Among the studies addressing river bank erosion and its impact on the morphology of the river channel and banks are the following:

- Aql (2003), conducted a study titled *"Erosion and Collapse and Their Impact on the Morphology of the Nile Banks between Kom Ombo and Esna: A Morphological Study"*, which analyzed the effects of erosion and collapse on the shaping of river banks in this segment of the Nile.
- El-Khayyat (2017), investigated "Bank Erosion and Collapse along the Nile River between Esna and Nag Hammadi Barrages: A Geomorphological Study Using GIS and

Remote Sensing". The study used GIS and remote sensing technologies to monitor bank changes and analyze some of the geomorphological factors responsible for those changes.

- Ahmed (2019), in his study "Geomorphology of Erosion and Deposition along the Nile River banks: Assiut Governorate", focused on analyzing geomorphological processes affecting the banks, particularly vertical and lateral erosion and deposition, and how these processes influence the morphological characteristics of the river channel.

4. Study Objectives

- Employing Geographic Information Systems (GIS) and Remote Sensing (RS) techniques to monitor and analyze the morphological changes that have occurred in the Nile River channel and its river islands following the construction of the High Dam, thereby contributing to an understanding of river bank dynamics and their temporal development.
- Analyzing and assessing the impact of hydrological characteristics on the dynamics and stability of river banks in the stretch between Matai and Al-Fashn.
- Examining the hydro-mechanical properties of river bank soils to understand their behavior under the influence of hydrological changes resulting from the High Dam, with the aim of explaining erosion and deposition mechanisms and identifying the most vulnerable bank segments in the study area.
- Classifying hazard levels of Nile River bank soils based on an integrated analysis of their hydro-mechanical properties and their sensitivity to fluctuating hydrological conditions.
- Identifying appropriate preventive and reinforcement measures to enhance river bank stability and mitigate the risks of collapse.

To achieve these objectives, the study tackled the following topics:

5. Channel Dynamics and Morphological Changes in the Study Area

The study of the morphological characteristics of the river channel and its islands serve as a fundamental approach to understanding the dynamics of the fluvial system. Analyzing these changes provides a basis for interpreting the behavior of the river within the study area. The morphological transformations that have occurred in the Nile River channel over recent decades reflect direct responses to multiple pressures, including both natural and anthropogenic factors, in addition to the pronounced influence of hydrological characteristics in shaping the river's course and behavior. These transformations serve as early indicators of instability or potential hazards, as they help explain the patterns of change in the river's course and its interaction with the surrounding natural and hydrological environment. By tracing the historical development of the Nile River channel in the study area from 1953 to 2023, it becomes possible to attain a more accurate understanding of the hydrological characteristics and their direct impact on river bank stability, as well as to identify areas most vulnerable to erosion and collapse.

5.1. Morphological Characteristics of the River Channel:

5.1.1. Channel Orientation

It is evident from (Figure 1) that the Nile River channel enters the study area at latitude 28°22′ N, approximately 3.75 km south of Kafr Al-Kawadi (Matai District). The channel initially flows northeastward to latitude 28°27′ N near Ezbet El-Salam, covering a distance of approximately 17.84 km. The river then shifts northward for 2.80 km to latitude 28°29′ N, after which it deviates sharply to the northwest until it reaches latitude 28°30′ N, west of Beni Mazar City, traversing a distance of 3.65 km. Next, the channel heads northeast until it reaches 28°34′ N near Al-Jarabi, covering 7.55 km, and continues northward for 8.51 km until 28°38′ N, south of Maghagha. It then veers northeast again, approaching the eastern escarpment of the Nile Valley until 28°47′ N west of Al-Qadabi, crossing 17.9 km. A subsequent northwestward deviation for 3.30 km occurs west of El-Sheqar village,

after which the river shifts northeast again, flowing closely along the eastern escarpment until 28°50′30″ N, north of Ezbet Deir Al-Hadid, over a distance of 4.44 km. From this analysis, it is evident that the northeast direction dominates the channel's course, extending over 51.48 km or approximately 73.8% of its total length. This is followed by the northward direction, which accounts for 11.31 km (16.2%). The dominance of the northeast direction can be attributed to two main factors:

- Climatic Factors: Predominantly northerly and northwesterly winds contribute to driving surface waters eastward, increasing erosion on the eastern bank and resulting in gradual eastward migration of the channel. However, the presence of the eastern limestone plateau, composed of hard rock formations (Figure 2), acts as a natural barrier, restricting this migration in certain segments.
- Structural (Tectonic) Influence: The river's course aligns with dominant fault trends in the region, especially those in a northeast-southwest orientation, which represent approximately 44.94% of total fault lengths in the area (Table 1). This clearly demonstrates the role of tectonic structures in guiding the channel's path through the bedrock configuration of the study area (Figure 2).

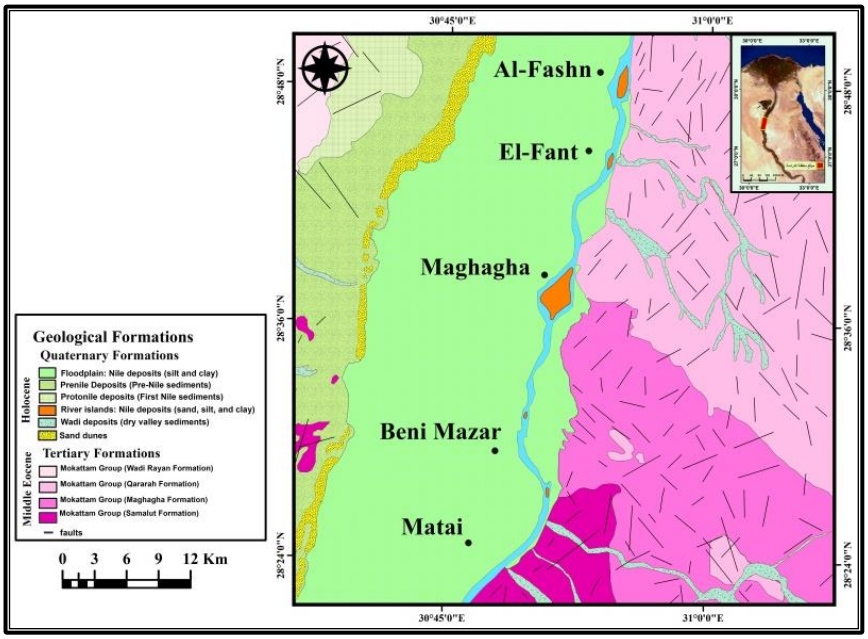

Source: Prepared by the researcher based on Beni Suef Geological Map (NH 36 SW, 1:500,000) by EGPC & Conoco Coral (1987), processed using ArcGIS 10.8.

Figure 2. Geological Map of the Study Area.

Table 1. Fault Trends and Their Lengths in the Study Area.

Fault Trend Direction	(N–S)	(E–W)	(NE–SW)	(NW–SE)	Total
Number of Faults	33	3	75	58	169
Total Fault Lengths (km)	77.41	10.39	179.59	132.23	399.63
Percentage of Faults (%)	19.53	1.78	44.38	34.32	100
Percentage of Fault Lengths (%)	19.37	2.60	44.94	33.09	100

Source: the Geological Map of Beni Suef Sheet (Scale 1:500,000), EGPC & Conoco Coral, 1987, processed using ArcGIS 10.8.

.5.1.2. Main Channel Length

The length of the main river channel is considered one of the most significant morphometric characteristics that reflect the geomorphological nature of a river. It serves as an effective indicator for tracing channel sinuosity and evaluating the dynamics of processes influencing the channel, such as erosion and deposition. Studying the channel length is crucial due to its strong relationship with hydrological factors that contribute to altering the river course and the temporal changes that affect its length over time, which in turn directly impacts river bank stability. An analysis of the data in (Table 2 & Figure 3), which document morphological changes in the Nile River channel between 1953 and 2023, reveals a notable increase in the channel length following the construction of the High Dam. In 1953, the channel measured approximately 67.2 km, while satellite imagery from 2023 shows an increase to 69.74 km, marking a growth of 2.54 km. This increase in the main channel length is attributed to several factors, including the intensified lateral erosion along the concave banks of meanders, which occurred simultaneously with sediment deposition on the convex sides. In addition, erosion along the eastern banks of straight channel segments also contributed to this lengthening. Another contributing factor is the attachment of some islands to one of the river banks—such as the merger of Mostafa El-Demerdashy and El-Sheikh Fadl islands with the eastern bank of the channel (Figure 4). Moreover, data in (Table 2) indicate a slight but consistent increase in the main channel length during the period from 1991 to 2023. This change is mainly attributed to the reduction in the river's flow velocity following the construction of the High Dam. The decreased kinetic energy reduced the effectiveness of vertical erosion, while enhancing lateral erosion, which in turn led to increased sinuosity in the river course and a gradual extension of its overall length. Moreover, the data in (Table 2) indicate a gradual, albeit slight, increase in the channel length between 1991 and 2023. This trend is likely due to a reduction in the river's flow energy following the dam's construction, which resulted in decreased vertical erosion and increased lateral erosion. This shift has led to greater channel sinuosity, and thus a gradual extension in the total length of the main channel.

Table 2. Morphological Changes of the Nile River Channel in the Study Area between 1953 and 2023

Sector	Study Years	Main Ch. Length (km)	Str. Ch. Length (km)	Riverbank Lengths (km)		River Channel Width (m)			Water Surface Area (km²)	Channel Perimeter (km)	Sinuosity Index (Brice, 1964)		Channel Depth (m) 2003		Long. Riv. Gradient (cm/km), 2003, Al-Fashn	Local Gradient (cm/km)
				E. Bank L. (km)	W. Bank L. (km)	Max. Ch. Width (m)	Max. Ch. Width (m)	Avg. Ch. Width (m)			Sinuosity Index (Brice, 1964)	Channel Pattern	Avg. Ch. Depth (m), Max. Disch. (174.06 MCM/d, Assiut Barrage)	Avg. Ch. Depth (m), Min. Disch. (65.44 MCM/d, Assiut Barrage)		
Matai - Al-Fashn	1953	67.200	61.31	70.78	74.18	3920	680	2300	50.07	146.12	1.096	Sinuosity	5.62	4.37	10	8.5
	1991	68.33	61.76	71.38	76.39	2480	394.76	1437.38	30.99	148.73	1.106	Sinuosity				
	2002	68.92	62.11	72.43	77.89	2310	225	1267.5	26.64	136.21	1.110	Sinuosity				
	2023	69.74	62.32	72.86	78.11	2290	170	1230	23.88	133.05	1.119	Sinuosity				
	Average	68.55	61.88	71.86	76.64	2750	367.44	1558.72	32.89	141.03	1.11	Sinuosity				
	Morphological Changes of the River Channel Between 1953 and 2023															
	1953-2023	2.54	1.01	2.08	3.93	-1630	-510	-1070	-26.19	-13.07	–		–		–	

Source: Topographic maps (1953, 1991), hydro-topographic maps (1980, 2003, 2007), and Landsat TM satellite scenes (2002, 2023; 30 m resolution), using data from EGSA, NWRC, and USGS, processed using ArcGIS 10.8.

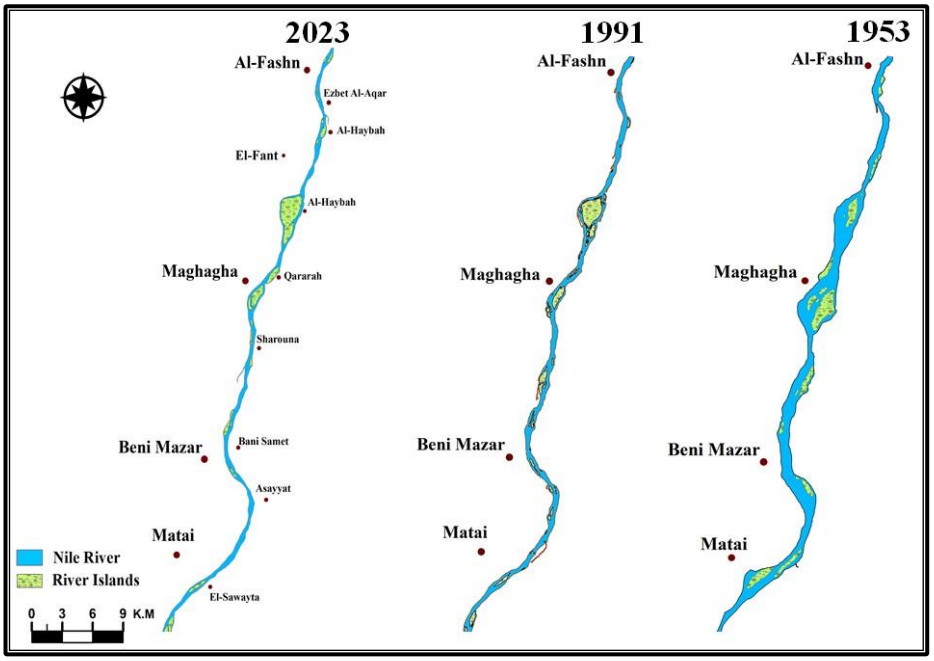

Source: Prepared by the researcher using ArcGIS 10.8, based on topographic maps (1953, 1991) and Landsat TM satellite scenes (2023; 30 m resolution), obtained from EGSA and USGS.

Figure 3. Morphological Changes of the Nile River Channel in the Study Area between 1953 and 2023

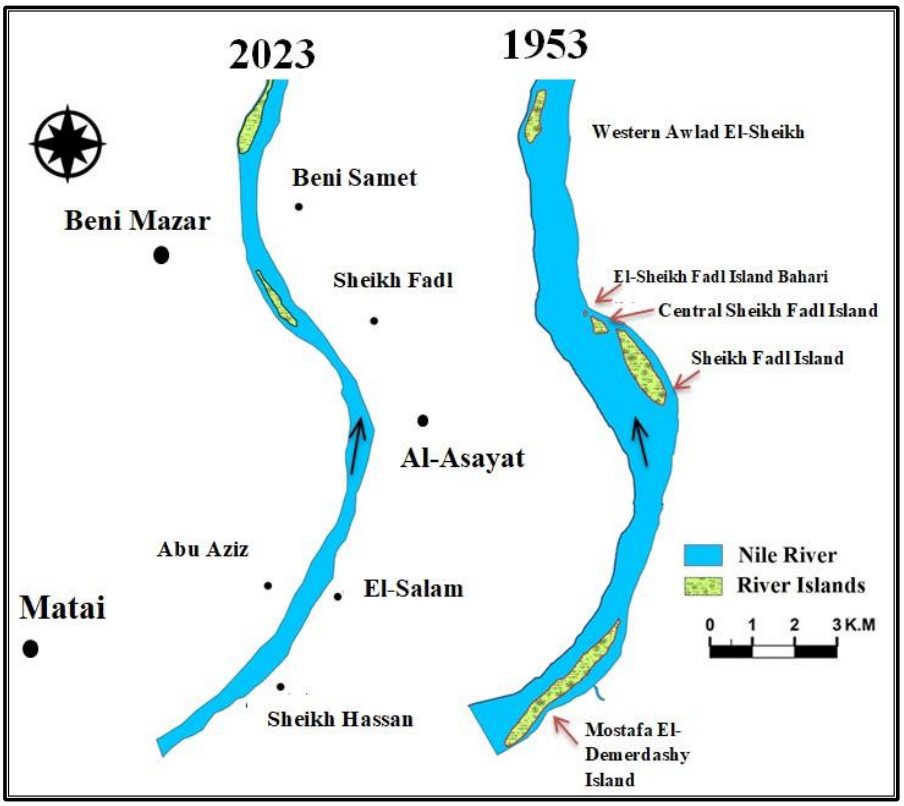

Source: Topographic maps (1953) and Landsat TM satellite scenes (USGS, 2023; 30 m resolution), processed using ArcGIS 10.8.

Figure 4. Increase in Main Channel Length in the Matai–Beni Mazar Reach Based on 2023 Imagery, Resulting from Enhanced Channel Sinuosity Associated with the Attachment of River Islands to the Eastern Bank

5.1.3. River Channel Width

The width of the river channel is one of the key morphometric characteristics that underwent significant morphological changes following the construction of the High Dam. In 1953, the average channel width was approximately 2,300 m, whereas it decreased to around 1,230 m in the 2023 satellite imagery, as shown in (Table 1). This represents a substantial reduction of approximately 53.48% compared to the 1953 measurement. This change is primarily attributed to several factors, notably the attachment of river islands to the channel banks, which led to their incorporation into the floodplain and subsequently reduced the overall channel width. Additionally, the increase in vertical erosion rates, relative to lateral erosion, played a crucial role. These processes are closely linked to the reduced river discharge and the decline in suspended sediment load following the construction of the High Dam. As a result, the river's available energy became more focused on deepening the channel bed rather than widening it. This is consistent with the study of Obaido (1982), which found that the effectiveness of fluvial erosion largely depends on discharge volume, flow velocity, and the suspended sediment load. The second factor involves human interventions in the secondary channels, where some farmers have contributed to filling these channels either by constructing earthen dams or by dumping agricultural waste. This has led to bed level aggradation and redirected water flow toward the main channel, which in turn has caused several islands to merge with the alluvial fabric of the floodplain. A notable example of this type of change is the secondary channel west of the western branch of Deir Al-Hadid Island, where the construction of a local earthen dam by residents has resulted in the partial attachment of the island to the floodplain, as shown in Figure 5. Furthermore, Table 1 shows that the channel has experienced a slight, gradual decrease in its average width during the period from 1991 to 2023. This can be attributed to the river's tendency to reach a state of hydraulic equilibrium under relatively stable conditions, which drives the channel to gradually adjust its morphology in accordance with the available energy budget.

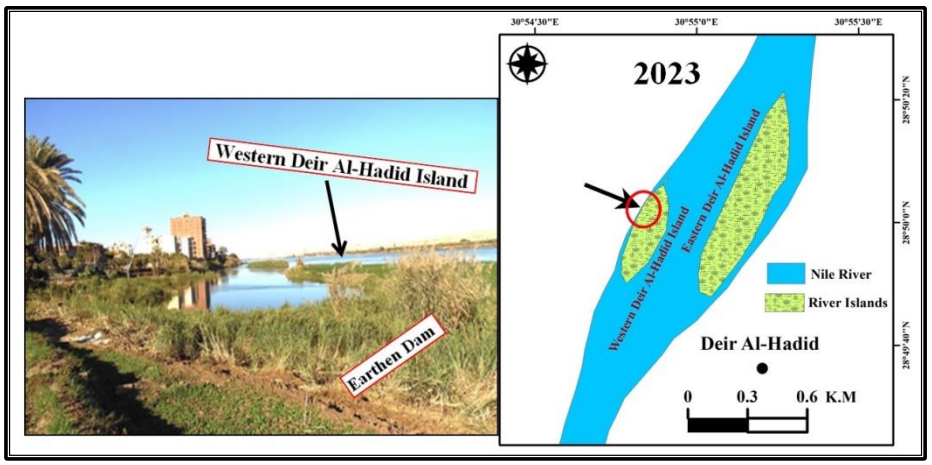

Source: Field Study, 2025 and Landsat TM satellite scenes (2023; 30 m resolution) obtained from USGS, processed using ArcGIS 10.8.

Figure 5. The Secondary Channel West of Deir Al-Hadid Island Experienced Siltation in Some Parts Due to the Construction of a Local Earthen Dam by Residents, Which Contributed to the Partial Attachment of the Island to the Adjacent Floodplain.

5.1.4. River bank Lengths

The lengths of the river banks within the study area have shown a notable gradual increase over the period from 1953 to 2023, as presented in Table 1. The length of the eastern bank ranged from 70.78 km in 1953 to 72.86 km in 2023, marking an increase of 2.08 km, equivalent to a 2.94% change. Similarly, the western bank exhibited a significant increase, extending from 74.18 km in 1953 to 78.11 km in 2023, representing a growth of 3.93 km and a

percentage change of 5.30%. Average values throughout the study period indicate that the western bank consistently exceeded the eastern bank in length, averaging approximately 76.74 km compared to 71.86 km for the eastern bank—a mean difference of 4.78 km. This disparity is attributed to several key factors, most notably the merging of a number of islands into the western floodplain as a result of continuous sedimentation in secondary channels, and human interventions such as the infilling of some of these channels. These factors have contributed to changes in the flow path and the extension of the actual river bank line. The general trend line equations ($y = 0.0307x + 10.69$ for the eastern bank, and $y = 0.05967x - 42.21$ for the western bank) indicate a steady increase in the lengths of both banks over the study years, reflecting the river's ongoing effort to re-establish morphological equilibrium in its banks under the combined influence of natural processes and human activities affecting the channel.

5.1.5. Water Surface Area

The decline in water surface area represents one of the most prominent morphometric characteristics of the Nile River channel within the study area, particularly following the construction of the High Dam. According to the data in Table 1, there has been a gradual reduction in the water surface area between 1953 and 2023. In 1953, the area measured approximately 50.07 km², which decreased to 30.99 km² in 1991, further declined to 26.64 km² in 2002, and ultimately reached 23.88 km² in 2023. This represents a total loss of 26.19 km², equivalent to a 52.3% reduction compared to the 1953 area. These figures indicate clear spatiotemporal changes in the extent of the water surface. Field investigations and satellite imagery analysis for 2023 reveal that the receded water surface areas have transformed into lands adjacent to the current river channel. This shrinkage can be attributed to a combination of factors, most notably the attachment of river islands to one of the river banks—such as the case of Sheikh Ibrahim Sharqiya Island joining the eastern bank (Section 3, Figure 6). Additional contributing factors include the increased rates of sedimentation and the emergence of river islands, particularly on the western side of the river. This pattern is largely influenced by local climatic conditions, where northern and northwestern winds prevail with frequencies of 48% and 18.2%, respectively (Atya, A., 2019, p. 21). These winds tend to push the water eastward, in alignment with Ferrel's Law, which states that moving objects in the Northern Hemisphere deviate to the right due to Earth's rotation (Emerson, 1919, p. 242). As a result, current velocity increases along the eastern bank and decreases on the western bank, fostering conditions for deposition and island formation in the west, thereby reducing the overall water surface area—as illustrated in Sections 1, 2, and 3 (Figure 6). The general trend line equation ($y = -0.3910x + 811.93$) reveals a consistent annual decrease of approximately 0.391 km² throughout the study period. This trend reflects the gradual recession of the water surface due to the aforementioned natural and anthropogenic factors, leading to a loss of more than half of the river's water surface area over 70 years.

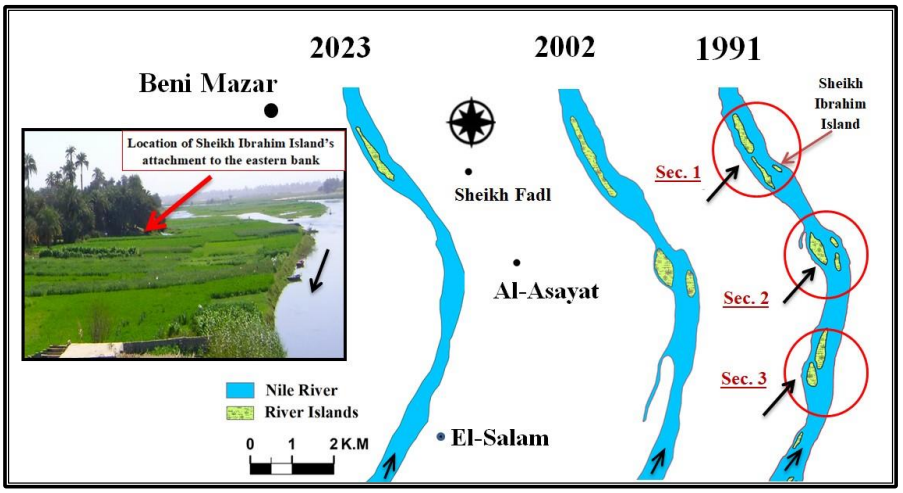

Source: Field Study, 2025, Topographic maps (EGSA, 1991), and Landsat TM satellite scenes (USGS, 2002, 2023; 30 m resolution), processed using ArcGIS 10.8.

Figure 6. Reduction of water surface area due to the attachment of river islands to one of the river banks

5.1.6. River Channel Perimeter

The perimeter of the river channel is considered one of the most significant morphometric variables that reflect the overall shape of the watercourse and the extent to which it is affected by erosion and deposition processes. An increase in channel perimeter typically indicates a higher number of meanders and the presence of abandoned secondary channels. Analysis of topographic maps and satellite imagery from 1953 to 2023 (Table 1) reveals a notable decrease in the perimeter of the Nile River channel within the study area. In 1953, the channel perimeter measured approximately 146.12 km. It then recorded a slight increase in 1991, reaching 148.73 km, likely due to the presence of several abandoned secondary channels. However, the subsequent years showed a consistent declining trend, with the perimeter measuring 136.21 km in 2002 and further decreasing to 133.05 km in 2023—representing a total reduction of 13.07 km compared to 1953. This decline is directly related to the reduction in water surface area, given the positive correlation between these two variables. Several key factors contribute to this decrease. One major factor is the attachment of some river islands to one of the river banks, such as the case of AL-Jarabi and El-Gondia islands, which became connected to the eastern bank. This shift caused the main water mass to move from the secondary channels to the primary channel, thus reducing both the water surface area and the overall perimeter of the river channel (Figure 7). Another contributing factor is the siltation of abandoned secondary channels, which also reduces the channel perimeter—for example, the abandoned channel east of El-Gondia village that experienced significant siltation (Figure 7).

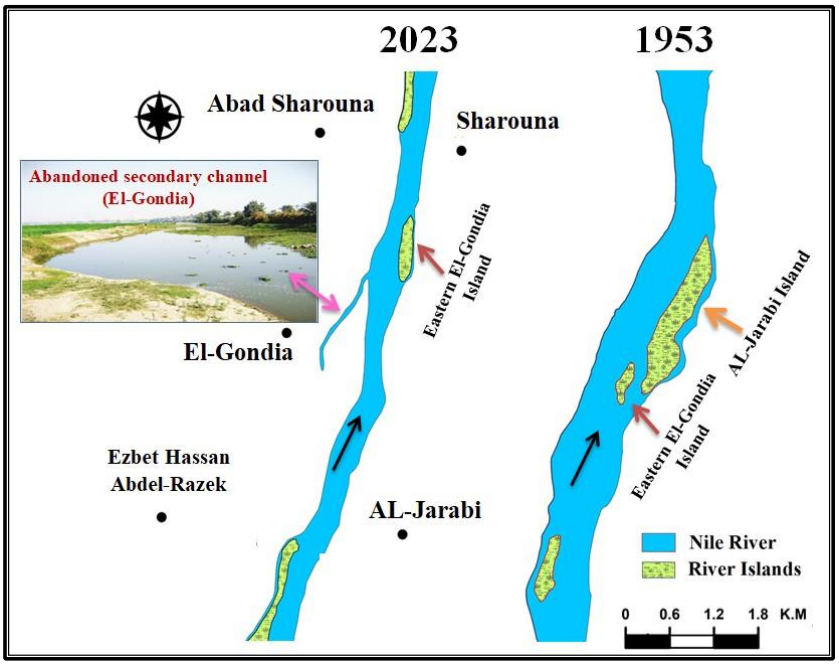

Source: Field Study, 2025, Topographic maps (ESA, 1953), and Landsat TM satellite scenes (USGS, 2023), processed using ArcGIS 10.8.

Figure 7. Reduction of water surface area and perimeter due to the attachment of AL-Jarabi and El-Gondia Islands to the eastern bank of the river channel

5.1.7. River Channel Pattern

The river channel pattern refers to the nature of the watercourse in terms of its linearity or sinuosity. Among the most widely used metrics for measuring channel sinuosity is the Brice Index (Brice, 1964). Applying this index to the Nile River within the study area over the period 1953–2023 (Table 1) reveals that the river has consistently exhibited noticeable sinuosity throughout the study period. In 1953, the sinuosity index was 1.096, increasing to 1.119 in the 2023 satellite imagery. These values indicate a moderately sinuous channel with a relatively stable pattern over time—comparable to the average sinuosity index of the Nile River across Egyptian territory, which has been estimated at 1.4 according to Brice's classification (Brice, 1964). This trend reflects a general morphological stability in the channel pattern, despite the influence of various geomorphological processes—most notably lateral erosion—as well as the attachment of river islands to one of the banks. These factors have contributed to slight modifications in the river course without causing substantial changes in its overall sinuosity over time.

5.1.8. River Channel Braiding

The study of river channel braiding is an essential tool for understanding how water and sediment are distributed within the watercourse and for predicting the river's behavior over time. Braiding often arises when islands obstruct the flow of water, and it is measured as the proportion of the river's length occupied by islands (El-Husseiny, 1991, p. 67). In this study, a number of morphometric equations and indicators were applied to measure channel braiding, most notably the Braiding Index proposed by Brice (1964, p. 30)[1]. The results showed that the river channel within the study area has not yet reached a fully braided stage throughout the 70-year study period. The braiding ratio was 0.95 in 1953, then declined to 0.79 in 2023. Moreover, when applying the braiding index according to El-Husseiny (1991, p. 68)[2] (Table 3), a clear decline

[1] Braiding Index = (Total Length of Islands [km] × 2) / Main Channel Length [km] (Brice, 1964, p. 30)
[2] Channel Braiding Ratio (%) = (Total Length of Secondary Channels [km] / Main Channel Length [km]) × 100 (El-Husseiny, 1991, p. 68)

in values was observed from 1953 to 2023, particularly after the construction of the High Dam. The index value dropped from 48.23% in 1953 to 40.33% in 2023, meaning that for every one kilometer of the main river course, there are approximately 403 m of secondary or distributary channels. This noticeable decline is primarily attributed to the siltation and disappearance of many secondary channels, caused by the attachment of several river islands to one of the river banks. Therefore, the braiding index offers a more accurate quantitative expression of river braiding, as it considers the actual lengths of secondary channels rather than merely the number or size of islands.

Table 3. Bifurcation of the Nile River channel between Matai and Al-Fashn during the period from 1953 to 2023

Sector	Study Years	Main Channel Length (km)	Islands – total length (km)	econdary channels – total length (km)	Bifurcation Index (Brice, 1964) (Total length of islands × 2) / Main channel length	Bifurcation Index (El-Husseiny, 1991) (Total length of secondary channels / Main channel length) × 100
Matai – Al-Fashn	1953	67.20	31.888	32.413	0.95	48.23
	1991	68.33	39.449	40.251	1.15	58.91
	2002	68.92	30.867	30.940	0.90	44.89
	2023	69.74	27.429	28.122	0.79	40.33

Source: Topographic maps (1953, 1991) and Landsat TM satellite scenes (2002, 2023; 30 m resolution), using data from EGSA and USGS, processed using ArcGIS 10.8.

5.1.9. Longitudinal Profile

The longitudinal profile of the Nile River channel between Matai and Al-Fashn is characterized by noticeable irregularity and ruggedness, stemming from the variability in bed elevations (Figure 8). According to Table 4, the average elevation difference between the highest and lowest points of the river bed is approximately 10.04 meters, indicating a significant disparity in channel bed topography. These longitudinal fluctuations recur at intervals of roughly 2.75 km, typically corresponding to lower bed segments located along the eastern bank in straight reaches, and along the concave banks within meandering sections. This spatial distribution is primarily attributed to variations in water flow velocity, direction, and differential erosion–deposition processes, which contribute to channel deepening in specific locations and the formation of such topographic undulations. The profile also exhibits relatively elevated portions of the river bed that lie close to the water surface during low-flow periods, with a vertical separation as little as 0.48 m, signifying shallow channel conditions in those zones. These shallow segments may negatively impact flow efficiency and hydraulic energy distribution, as observed near kilometer marker 757.5 km north of the Aswan Reservoir (Figure 8). Table 4 further reveals substantial topographic variability along the river bed between Matai and Al-Fashn. During maximum discharge conditions, water depths range from 1.81 to 10.52 m, with an average of 5.36 m. Under minimum discharge, depths vary from 0.48 to 9.47 m, averaging 4.18 m. The channel's longitudinal gradient is relatively steep—approximately 10 cm/km, significantly higher than the gradient measured in the Assiut –Cairo reach, which averages 7.5 cm/km (El-Husseiny, 1988, p. 8). The ruggedness and steep gradient of the river bed are attributed to a combination of hydromorphological factors, primarily the variation in erosion and sedimentation rates along the channel, particularly at meander bends. Additionally, the attachment of river islands to one of the banks redirects water flow toward the main channel, increasing current velocity and prompting the river to reshape itself through enhanced lateral and vertical erosion in pursuit of a new state of equilibrium. Human interventions—such as the infilling of secondary channels—also play a role by forcing water into the main channel, thus

intensifying erosion processes. Lastly, the frontal portions of islands, directly exposed to current flow, experience more pronounced erosion, while the rear parts remain relatively sheltered (Salama, 2006, p. 108).

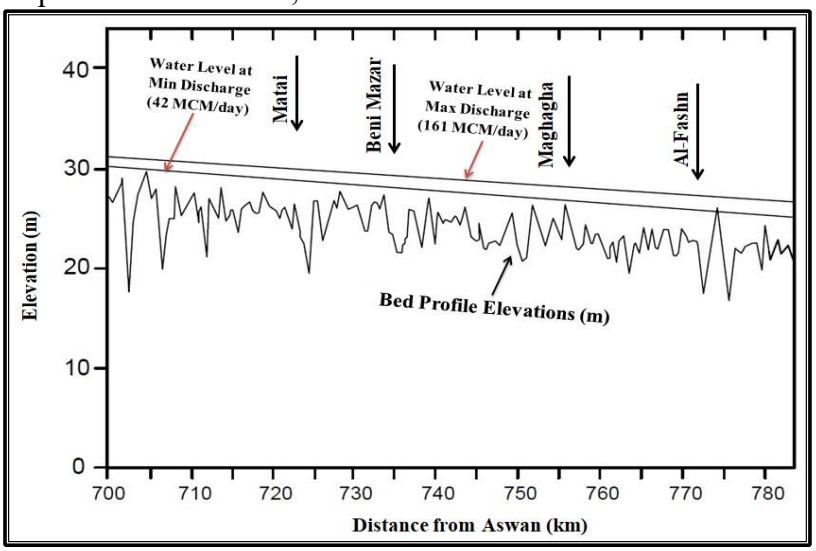

Source: Nile Research Institute, longitudinal profile of river bed elevations, unpublished data, 2003. Redrawn using AutoCAD Map 3D 2019.

Figure 8. Variation in Bed Elevation along the Nile River Channel from Matai to Al-Fashn

Table 4. Channel Depth between Matai and Al-Fashn based on Water Discharges Passing Downstream of Assiut Barrage in 2003

Distance (km) from Aswan Dam	Channel Depth (m) at Max Discharge (161 MCM/day), Assiut Barrage, 2003	Channel Depth (m) at Min Discharge (42 MCM/day), Assiut Barrage, 2003	Point
705	2.16	1.44	South of Al-Kawadi — West of the Nile
707.5	2.88	2.16	Kafr Al-Kawadi — West of the Nile
710	6.12	5.4	North of Kafr Al-Kawadi — West of the Nile
712.5	2.88	2.16	Al-Asayat— East of the Nile
715	6.84	6.12	North of Al-Asayat — East of the Nile
717.5	4.68	3.24	Nazlat Abu Shahata — West of the Nile
721	4.53	3.13	Sheikh Hassan — East of the Nile
723	9.90	8.89	Matai — West of the Nile
725	10.32	9.47	Kafr Al-Sawaleya — West of the Nile
727	3.30	2.02	Kafr Sheikh Ibrahim — West of the Nile
730	3.21	2.46	Nazlat Dalil — West of the Nile
734	2.92	1.68	Sheikh Fadl — East of the Nile
735	7.80	6.80	Beni Mazar — West of the Nile
738	3.28	1.45	Beni Samet — East of the Nile
740	3.56	2.41	Beni Samet — East of the Nile
741	4.23	3.05	Al-Jarabi‘ — West of the Nile
742.5	4.26	3.25	Al-Nasiriya — East of the Nile
745	2.95	1.72	El-Gondia — East of the Nile
747.5	6.45	5.19	El-Gondia — East of the Nile
750	7.69	6.48	South of Sharuna Island
752.5	4.97	3.59	Abad Sharouna — West of the Nile
755	4.62	3.29	Sheikh Ziyad — West of the Nile
757.5	1.81	0.48	Maghagha — West of the Nile
760	5.02	3.69	Azbat Al-Sa‘ayda — West of the Nile
762.5	6.74	5.15	Zawiyat Al-Gidami — East of the Nile
765	5.51	4.28	Al-Fant — East of the Nile
767.5	5.62	4.23	Al-Haybah — East of the Nile
770	6.03	4.66	Azbat Al-Aqr — East of the Nile
772	10.52	8.96	Al-Fashn — West of the Nile
774.7	9.85	8.63	Deir Al-Hadid — East of the Nile
Avg. Depth (m)	5.36	4.18	——

Source: Water depth was calculated based on Table 4 using AutoCAD Map 3D 2019, from the longitudinal profile of the Nile River channel bed elevations (Nile Research Institute, unpublished data, 2003).

5.1.10. River Meanders

River meanders represent one of the most prominent morphological features of fluvial systems. They are curvatures in the river course that originate and evolve through a complex interplay of natural and hydrological factors. These include the geological structure of the terrain through which the river flows, the physical properties of channel bed and bank materials, channel gradient, flow velocity, and the presence of natural obstructions such as river islands. Moreover, variations in the intensity and dominance of erosion and deposition processes—both lateral and vertical—play a decisive role in the formation and progressive development of meanders over time.

An analysis of Table 5 reveals the following key findings:

- Three major river meanders were identified in the reach between Matai and Al-Fashn, with an average spacing of one meander every 23.24 km. These include Al-Asayat, El-Gondia, and Zawiyat Al-Gidami. These meanders experienced distinct morphological changes during the study period (1953–2023), marked by a gradual increase in their lengths following the construction of the High Dam. In 1953, the total meander length was 51.29 km, accounting for 76.33% of the main river course, which increased to 51.71 km or 77.59% in 2023. This trend reflects a steady pattern of morphological development. The relative consistency in average lengths between 1991 and 2023 indicates a state of morphometric stability, reflecting a dynamic equilibrium between erosion and deposition in recent decades.
- The average lengths of river meanders within the study reach varied significantly during the 70-year period, ranging from 17.10 km in 1953 to 18.04 km in 2023. This change can be attributed to sustained erosion and sedimentation activity—particularly at meander inlets and outlets—as well as transformations in the morphology of river islands, whether through attachment to the river banks or the formation of new islands. For instance, the length of Al-Asayat meander increased from 16.89 km in 1953 to 19.22 km in 1991, a difference of 2.33 km. The data further show a relative stabilization in average lengths between 1991 and 2023, suggesting that the meanders have entered a phase of morphodynamic equilibrium, coinciding with more regular flow regimes since the 1990s.
- The lengths of meander axes in the Matai–Al-Fashn sector also displayed clear morphological variability during the study period, ranging between 15.34 km and 16.24 km. This variation results from cumulative geomorphological processes—particularly erosion and deposition at meander entrances and exits—as well as shifts in island morphology, including both island attachment and emergence. For example, the length of Al-Asayat's axial line increased from 16.89 km in 1953 to 19.22 km in 1991, with a 2.33 km increase. Topographic maps from 1991 attribute this change to two key factors: (1) the attachment of the islands "Tallat Abu Shuhata" and "Mostafa El-Demerdashy" at the inlet of the meander, as well as "West Awlad El-Sheikh Island" at its outlet; and (2) the formation of new river islands at the meander's exit, including "Sheikh Fadl Bahariyya," "Nazlat Dalil Qibliyya," "Beni Mazar," "Beni Samet," "Awlad El-Sheikh," and "Awlad El-Sheikh Sharqiyya" (Figure 9).
- There is notable variation in the average channel width at meander locations throughout the study period (1953–2023), ranging from 0.449 km in 1953 to 0.543 km in 2023, reflecting an overall increase of 0.094 km or approximately 20.9%. This change is attributed to the river's ongoing effort to achieve hydromorphological equilibrium through processes such as island accretion, island emergence due to fluvial activity, or the merging of multiple islands into a single landmass. These interpretations are supported by the data in Table 5, which show significant variation in the number and size of river islands over time—factors that contribute directly to reshaping the channel width within meander zones and underscore the dynamic nature of the river system as it responds to shifting hydrological and geomorphological conditions.

Table 5. Morphological Changes of River Meanders in the Study Area during the Period from 1953 to 2023.

Sector	Study Years	Meander Name	Actual Meander Length (km)	Meander Axis Length (km)	Channel Width in Meanders (km)	Meander Belt Width (km)	Radius of Meander Curvature (km)	River Islands within Meanders		Meander Sinuosity (Brice,1964)		Meander Length / Axis Length	Meander Length / Channel Width	Meander Length / Belt Width	Meander Length / Radius of Curvature	Radius of Curvature / Channel Width	Belt Width / Channel Width	Belt Width / Radius of Curvature
								Number of Islands	Island Area (km^2)	AverageSinuosity Ratio	Channel Pattern Average							
Matai – Al-Fashn	1953	Al-Asayat	20.21	16.89	0.645	4.72	2.20	6	3.44	1.20	Sinuous	1.20	26.19	4.28	9.19	3.41	7.32	2.15
		El-Gondia	10.80	10.15	0.440	2.39	1.13	6	2.03	1.06	Sinuous	1.06	24.55	4.51	9.56	2.57	5.44	2.12
		Zawiyat Al-Gidami	20.28	18.98	0.412	2.55	1.320	8	6.77	1.07	Sinuous	1.07	49.24	7.95	15.36	3.20	6.19	1.93
		Avg	**17.10**	**15.34**	**0.499**	**3.22**	**1.55**	**20**	**12.24**	**1.104**	**Sinuous**	**1.115**	**34.266**	**5.308**	**11.031**	**3.106**	**6.455**	**2.078**
	1991	Al-Asayat	22.28	18.91	0.598	5.22	2.42	20	1.56	1.18	Sinuous	1.18	37.24	4.27	9.21	4.04	8.73	2.16
		El-Gondia	11.48	10.73	0.682	2.54	1.29	8	1.57	1.07	Sinuous	1.07	16.85	4.52	8.90	1.89	3.73	1.97
		Zawiyat Al-Gidami	20.93	19.71	0.507	2.98	1.560	28	6.21	1.06	Sinuous	1.06	41.32	7.02	13.42	3.08	5.88	1.91
		Avg	**18.23**	**16.45**	**0.595**	**3.58**	**1.76**	**56**	**9.34**	**1.097**	**Sinuous**	**1.108**	**30.617**	**5.093**	**10.379**	**2.950**	**6.012**	**2.038**
	2002	Al-Asayat	22.30	19.16	0.552	5.48	2.77	7	1.27	1.16	Sinuous	1.16	40.38	4.07	8.05	5.02	9.92	1.98
		El-Gondia	11.42	10.59	0.562	2.76	1.59	6	2.28	1.08	Sinuous	1.08	20.33	4.14	7.18	2.83	4.91	1.74
		Zawiyat Al-Gidami	21.04	19.67	0.459	3.16	1.790	9	7.11	1.07	Sinuous	1.07	45.82	6.66	11.75	3.90	6.88	1.77
		Avg	**18.25**	**16.47**	**0.524**	**3.80**	**2.05**	**22**	**10.66**	**1.108**	**Sinuous**	**1.108**	**34.806**	**4.804**	**8.904**	**3.909**	**7.246**	**1.854**
	2023	Al-Asayat	22.14	19.22	0.482	5.97	2.91	3	1.31	1.15	Sinuous	1.15	45.91	3.71	7.61	6.03	12.38	2.05
		El-Gondia	11.35	10.18	0.659	2.94	1.98	7	1.22	1.12	Sinuous	1.12	17.22	3.86	5.73	3.00	4.46	1.48
		Zawiyat Al-Gidami	20.61	19.33	0.487	3.76	2.11	8	7.76	1.07	Sinuous	1.07	42.33	5.48	9.77	4.33	7.73	1.78
		Avg	**18.04**	**16.24**	**0.543**	**4.22**	**2.33**	**18**	**10.30**	**1.112**	**Sinuous**	**1.110**	**33.225**	**4.270**	**7.730**	**4.298**	**7.781**	**1.810**

Source: Topographic maps (1953, 1991) and Landsat TM satellite scenes (2002, 2023; 30m resolution) obtained from EGSA and USGS, processed using ArcGIS 10.8.

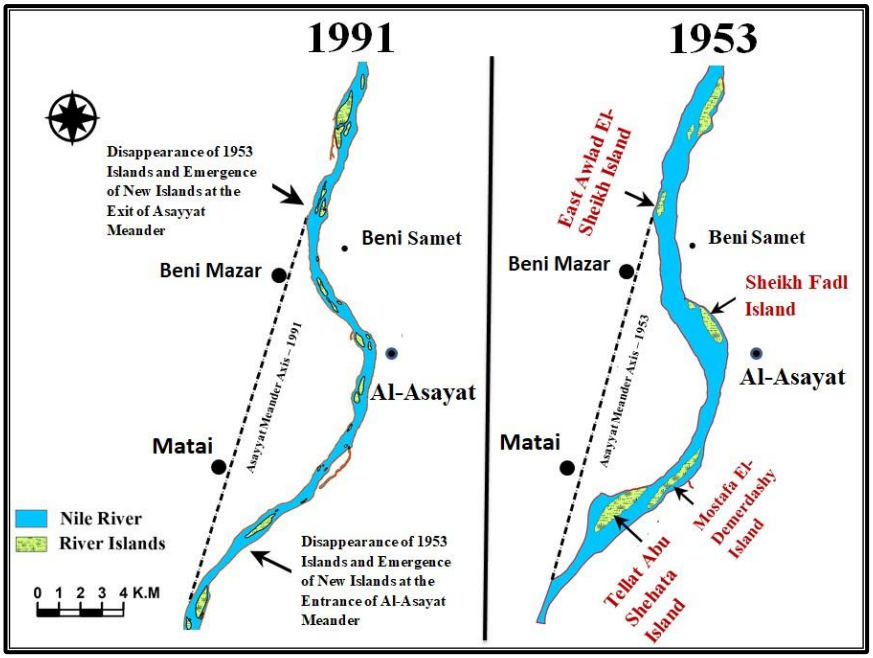

Source: Topographic maps (1953, 1991) from the Egyptian General Survey Authority (EGSA), processed using ArcGIS 10.8.

Figure 9. Variation in the Morphological Characteristics of Al-Asayat Meander during the Period (1953–1991)

- The average width of meander belts recorded a clear increase over the study period, ranging from 3.22 km in 1953 to 4.22 km in 2023 (Table 5). This expansion is primarily attributed to intensified erosion on the concave banks of meanders, which caused a migration of the meander belt toward the east and an overall widening of its spatial extent. A strong positive correlation was observed between meander belt width and the mean radius of curvature, with a correlation coefficient of 0.94. The average radius of curvature itself increased from 1.55 km in 1953 to 2.33 km in 2023, representing a

33.47% increase—indicating an elongation of the river course and a progressive extension of the meander forms.

- The ratios of meander length to channel width ranged between 30.62 and 34.81, far exceeding the typical range cited in the literature, which lies between 5 and 7 times the width. This unusually high ratio is attributed to the merging of a large number of river islands with the river banks following the construction of the High Dam, as well as the infilling of secondary channels by local farmers aiming to reclaim land for agriculture. These interventions have led to the integration of islands into the alluvial plain and significantly increased meander lengths.
- The ratios of meander length to meander belt width ranged from 4.27 to 5.31, which is consistent with values recorded in the Nile reach between Minya and Beni Suef (average = 4.4) (Desouki, 2002, p. 48). This suggests that some meanders in the study area—such as Al-Asayat and Zawiyat Al-Gidami—are relatively elongated in comparison to their belt width. Statistical analysis further revealed a strong positive correlation (r = 0.68) between these two variables (Table 6).
- The ratios of meander length to radius of curvature ranged between 7.73 and 11.03, which is close to the corresponding values reported for the Nile between Sohag and Assiut (Hegab, 2015, p. 26), where the range was 5.22 to 9.14. These values surpass the standard theoretical ratio of 4.7 suggested in earlier studies (Leopold & Langbein, 1966, p. 60). A moderate to strong positive correlation (r = 0.61) was also found between these variables (Table 6).
- The ratios of radius of curvature to channel width ranged from 2.95 to 4.30, aligning closely with the corresponding range for the Nile between Minya and Beni Suef 2 to 4.5, (Desouki, 2002, p. 49). In contrast, these values are considerably lower than those recorded for the Sohag– Assiut sector, which ranged from 6.15 to 56.2 (Hegab, 2015, p. 50). This disparity reflects variations in the morphometric properties of meanders across different Nile segments, underscoring the role of differing geomorphological and hydrological controls. A very strong positive correlation (r = 0.95) was identified between radius of curvature and channel width (Table 6), suggesting a close interdependence between these two variables.
- Among all measured variables, the radius of curvature emerged as the most influential factor in determining the morphometric dimensions of meanders within the study area, followed by meander belt width. This finding contrasts with that of (Desouki, 2002, p. 50), who identified meander axis length as the most impactful variable in the Minya–Beni Suef reach. However, it agrees with earlier conclusions by (Desouki, 1997, p. 76) regarding the Rosetta Branch, which highlighted radius of curvature as the primary controlling variable in meander morphology.

Table 6. Correlation Relationships among the Morphometric Dimensions of River Meanders.

Morphometric Dimensions of River Meanders	Actual Meander Length (km)	Meander Axis Length (km)	Channel Width in Meanders (km)	Meander Belt Width (km)	Radius of Curvature (km)
Actual Meander Length (km)	1	0.98	-0.31	0.68	0.61
Meander Axis Length (km)		1	-0.41	0.55	0.50
Channel Width in Meanders (km)			1	0.12	0.95
Meander Belt Width (km)				1	0.95
Radius of Curvature (km)					1

Source: Prepared by the researcher; correlation coefficients were calculated based on the data from Table 5 using Excel 2010 software.

5.2. Morphological Changes of River Islands

River islands serve as morphological archives that clearly reflect the hydrological activity of a river, both past and present. Their growth leads to increased channel braiding and generates heterogeneous hydraulic conditions that significantly influence channel structure and flow behavior. The number, distribution, and evolution of river islands are closely linked to the morphometric, hydrogeological, and geological characteristics of the river system (Baubinienė et al., 2015, p. 343), which are fundamental factors governing island genesis and transformation. Analysis of Table 7 reveals that the islands within the study area underwent notable morphological changes over the past 70 years, as follows:

- The number of river islands fluctuated significantly during the study period: from 20 islands in 1953, increasing to 60 in 1991, then decreasing to 24 islands in 2002, and reaching 21 islands by 2023. The spike in island numbers after the construction of the High Dam—most evident in the 1991 maps—can be attributed primarily to a substantial reduction in water discharge downstream of Assiut Barrage, which caused water levels to drop, revealing previously submerged landforms. A second factor is the sharp decline in suspended sediment load, which dropped from 134.428 Mt/yr in 1955 to 3.1 Mt/yr in 1977, representing a 97.69% decrease. This drastic reduction intensified flow velocities and enhanced both vertical and lateral erosion as the river system sought to re-establish a new state of dynamic equilibrium. These processes contributed to the formation of new islands, which appeared on the 1991 maps but soon disappeared in the 2002 satellite imagery, likely due to their merging with existing islands or the adjacent floodplain.
- The total area of river islands in the study area decreased by 1.79 km² between 1953 and 2023. In 1953, island areas totaled 12.823 km², with individual sizes ranging from 0.005 km² to 3.627 km², a mean of 0.616 km², and a standard deviation of 0.860. By 2023, the total area had decreased to 10.540 km², with areas ranging between 0.0002 km² and 5.312 km², a mean of 0.496 km², and a standard deviation of 1.140. A comparative analysis of the 1956 maps and 2023 satellite images (Table 8) shows that only four islands persisted throughout the 70-year period, while 16 islands merged with the alluvial floodplain, amounting to a total loss of approximately 4.911 km²—a clear indication that the river system has not yet achieved full geomorphic stability. Meanwhile, the 2023 imagery reveals the formation of 17 new islands, with a combined area of 3.416 km². The high standard deviation values for island size reflect a significant disparity in island dimensions, especially in the post-High Dam era.

Table 7. Morphological changes of the river islands in the study area during the period from 1953 to 2023

Morphometric Characteristics of River Islands		Study Years			
		1953	1991	2002	2023
Total Number of Islands		20	60	24	21
Island Area	Total Area (km²)	12.328	9.503	10.776	10.540
	Max Area (km²)	3.627	3.589	4.231	5.312
	Min Area (km²)	0.005	0.003	0.026	0.000
	Mean Area (km²)	0.616	0.158	0.449	0.496
	Std. Dev. (km²)	0.860	0.482	0.880	1.140
Island Lengths	Total Length (km)	31.888	39.449	30.867	27.429
	Max Length (km)	4.236	2.966	4.072	4.938
	Min Length (km)	0.093	0.077	0.300	0.031
	Mean Length (km)	1.594	0.657	1.286	1.306
	Std. Dev. (km)	1.264	0.595	0.985	1.083
Island Widths	Mean Total Width (km)	7.729	11.226	8.076	7.037
	Mean Max Width (km)	1.334	1.946	1.967	2.031
	Mean Min Width (km)	0.009	0.038	0.086	0.009
	Mean Avg. Width (km)	0.386	0.187	0.336	0.335
	Std. Dev. of Avg. Width (km)	0.302	0.260	0.382	0.423

Source: Topographic maps (1953, 1991) and Landsat TM satellite scenes (2002, 2023; 30 m resolution), using data from EGSA and USGS, processed using ArcGIS 10.8.

- River islands exhibited notable changes in their lengths throughout the study period. In 1953, the total cumulative length of the islands reached approximately 31.88 km, with individual lengths ranging from 0.039 km to 4.236 km, an average of 1.594 km, and a relatively high standard deviation of 1.264. This indicates a significant variance in island lengths at that time, reflecting diverse morphological shapes and spatial extensions. By 2023, the total length had declined to 27.429 km, with lengths ranging from 0.031 km to 4.938 km, an average of 1.306 km, and a lower standard deviation of 1.038. This reduction in standard deviation suggests a trend toward homogenization, with island lengths becoming more clustered around the mean—implying a narrowing of morphological variability in their longitudinal development.
- The average widths of river islands also varied across the study period, as shown in Table 7. In 1953, the sum of average widths was 7.729 km, with a mean width of 0.386 km and a standard deviation of 0.302, indicating moderate variability in island widths before the construction of the High Dam. By 1991, the total sum of average widths rose to 11.226 km, while the mean width decreased to 0.187 km, and the standard deviation increased to 0.336. This increase in the cumulative width is attributed to the sharp rise in island numbers, which reached 60 islands, resulting in greater dispersion in width values, especially due to the proliferation of numerous small-sized islands—hence the drop in the mean width. In the subsequent years, the total sum of island widths declined gradually, reaching 7.037 km in 2023, while the mean width increased again to 0.335 km, and the standard deviation rose to 0.402. These trends indicate a reduction in island numbers compared to 1991, accompanied by the emergence of relatively wider islands, which may reflect the merging of adjacent islands or the disappearance of smaller ones.

Table 8. Morphometric Comparison of River Islands between 1953 and 2023.

Island	Island Type	1953			2023		
		Area (km²)	Length (km)	Avg. Width (km)	Area (km²)	Length (km)	Avg. Width (km)
Al-Kawadi Island	Recent Formation	—	—	—	0.684	1.934	0.524
Tellat Abu Shehata Island	Persistent (Islands)	1.530	3.160	0.705	0.427	2.082	0.219
Mostafa El-Demerdashy Island	Integrated (Islands)	0.926	3.685	0.296	—	—	—
Sheikh Fadl Island	Persistent (Islands)	0.651	1.909	0.464	0.203	1.530	0.205
Central Sheikh Fadl Island	Integrated (Islands)	0.078	0.438	0.268	—	—	—
Sheikh Fadl Bahariyah Island	Integrated (Islands)	0.005	0.093	0.054	—	—	—
Beni Mazar Island	Recent Formation	—	—	—	0.485	2.461	0.348
Eastern Beni Mazar Island	Recent Formation	—	—	—	0.054	0.599	0.126
Western Awlad El-Sheikh Island	Integrated (Islands)	0.251	1.188	0.333	—	—	—
El-Gondia Bahariyah Island	Recent Formation	—	—	—	0.164	1.008	0.215
Eastern El-Gondia Island	Integrated (Islands)	0.115	0.771	0.202	—	—	—
AL-Jarabi Island	Integrated (Islands)	1.061	2.974	0.611	—	—	—
Abad Sharouna Qibliyah Island	Recent Formation	—	—	—	0.038	0.311	0.156
Abad Sharouna Island	Recent Formation	—	—	—	0.157	1.310	0.138
Abad Sharouna Bahariyah Island	Recent Formation	—	—	—	0.071	0.542	0.186
Sharouna Ferry Island	Recent Formation	—	—	—	0.253	1.279	0.224
Main Sharouna Island	Persistent (Islands)	3.627	4.236	1.334	1.181	2.298	0.737
Sheikh Zeyad Island	Integrated (Islands)	0.536	1.581	0.491	—	—	—
Central Sheikh Zeyad Island	Integrated (Islands)	0.061	0.404	0.159	—	—	—
Sheikh Zeyad Bahariyah Island	Integrated (Islands)	0.253	0.917	0.318	—	—	—
Maghagha Island	Integrated (Islands)	0.770	2.388	0.508	—	—	—
Qararah Island	Recent Formation	—	—	—	0.658	1.910	0.514
Main Zawiyat Al-Gidami Island	Persistent (Islands)	1.576	2.939	0.772	5.312	4.938	2.031
Zawiyat Al-Gidami Bahariyah Island	Integrated (Islands)	0.048	0.462	0.009	—	—	—
AL-Malatia Island	Integrated (Islands)	0.023	0.304	0.095	—	—	—
Al-Fant Qibliyah Island	Integrated (Islands)	0.387	2.297	0.274	—	—	—
Al-Fant Island	Integrated (Islands)	0.085	0.546	0.221	—	—	—
El-Fant Qibliyah Island	Recent Formation	—	—	—	0.083	0.693	0.171
Al-Haybah Qibliyah Island	Recent Formation	—	—	—	0.345	1.236	0.373
Western Al-Haybah Island	Recent Formation	—	—	—	0.064	0.556	0.205
El-Sheqar Qibliyah Island	Recent Formation	—	—	—	0.055	0.569	0.117
Central El-Sheqar Island	Recent Formation	—	—	—	0.062	0.517	0.146
El-Sheqar Bahariyah Island	Integrated (Islands)	0.156	0.790	0.292	—	—	—
Western Deir Al-Hadid Island	Recent Formation	—	—	—	0.060	0.531	0.167
New Deir Al-Hadid Island	Recent Formation	—	—	—	0.000	0.031	0.009
Deir Al-Hadid Island	Recent Formation	—	—	—	0.182	1.094	0.227
Totals		12.139	31.081	7.406	10.540	27.429	7.037
Averages		0.616	1.594	0.386	0.496	1.306	0.335

Morphometric Dimensions by Island Type

Island Type	Total Number of Islands	Area (km²)	Length (km)	Width (km)
Persistent (Islands)	4	7.124	10.848	3.191
Integrated (Islands)	16	4.911	19.627	4.422
Recent Formation islands (appeared in 2023 satellite views)	17	3.416	16.581	3.846

Source: Topographic maps (1953) and Landsat TM satellite scenes (USGS, 2023), processed using ArcGIS 10.8.

6. Spatial Analysis of Hydrological Factors Affecting the Stability of the Nile River banks in the Study Area

Hydrological factors are among the primary determinants shaping the course and banks of the Nile River within the study area. Their significance has increased considerably in light of the hydrological changes that followed the construction of the High Dam, which had a direct impact on the river's behavior and its natural balance. As a result, hydrological characteristics have come to play a more prominent role in reshaping the morphological form of the river. A spatial analysis of these factors highlights the extent of their influence on the degree of river bank stability, as they control the efficiency of water flow and its capacity to induce erosion and deposition processes, which in turn lead to morphological transformations within the river channel. These factors include water discharge volume, fluctuations in water levels, current velocity, and suspended sediment load—interrelated components that dynamically interact and collectively determine the behavior of the river and the vulnerability of its banks to erosion or sedimentation. This dynamic interplay constitutes a core element in interpreting the patterns of instability along the river banks in the study area.

6.1. Water Discharge

River discharge refers to the volume of water flowing through a specific point in the river channel over a given period of time (Strahler, 1964). It is considered one of the most critical hydrological factors governing river behavior, as it primarily determines the velocity of flow and

the river's capacity for erosion, deposition, and sediment transport. Moreover, it plays a direct role in reshaping river banks and in the formation or disappearance of river islands, depending on the dynamic capacity of the river associated with discharge volume. The marked decline in water discharge following the construction of the High Dam has had significant consequences, notably a reduction in the water surface levels within the channel. This has negatively impacted bank stability—particularly in areas where the river banks rise significantly above water level and are characterized by steep slopes—thereby increasing the likelihood of bank collapse due to turbulent eddies that cause localized disturbances and weaken the cohesion of bank soils.

An analysis of Table 9, which presents water discharge volumes downstream of the Assiut Barrage during the period 1968–2007, reveals significant variability in discharge levels across different years, as also illustrated in Figure 10. Minimum daily discharge ranged from 32 (MCM/day) in 1992 to 77 (MCM/day) in 1980—a difference of 45 MCM/day. Maximum daily discharge values varied between 127 (MCM/day) in 1988 and 182 (MCM/day) in 2001, marking a difference of 55 (MCM/day). The same table also indicates a notable difference between the average minimum and maximum discharge throughout the period, reaching approximately 103.38 (MCM/day). This wide variation in annual discharge volumes has resulted in recurrent fluctuations in water levels and flow velocities, contributing to a state of hydrological instability that adversely affects both the river's morphology and the stability of its banks.

Table 9. Water Discharges and Their Corresponding Water Levels Along the Nile River Channel in the Study Area During the Period from 1968 to 2007

Year	Min. Water Discharge (MCM/day)	Water Levels (m)				Max. Water Discharge (MCM/day)	Water Levels (m)			
		Dist. from Aswan Dam (km)					Dist. from Aswan Dam (km)			
		710	730	750	770		710	730	750	770
		Kafr Al-Kawadi	Nazlet Dalil	South of Sharouna Island	Ezbet Al-Aqar		Kafr Al-Kawadi	Nazlet Dalil	South of Sharouna Island	Ezbet Al-Aqar
1968	60	31.03	29.7	28.48	27.08	153	33.7	32.25	30.56	29.4
1970	63	31.23	29.82	28.6	27.2	148	33.02	31.57	30.68	29.52
1972	75	31.65	30.24	29.02	27.62	151	33.08	31.63	31.1	29.94
1974	65	31.19	29.78	28.56	27.16	138	32.92	31.47	30.64	29.48
1976	70	31.48	30.07	28.85	27.45	143	33.32	31.87	30.93	29.77
1978	61	31.04	29.63	28.41	27.01	163	33.32	31.87	30.49	29.33
1980	77	31.67	30.26	29.04	27.64	161	33.28	31.83	31.12	29.96
1982	73	31.59	30.18	28.96	27.56	158	33.22	31.77	31.04	29.88
1984	62	31.2	29.79	28.57	27.17	160	33.26	31.81	30.65	29.49
1986	42	30.91	29.5	28.28	26.88	159	33.24	31.79	30.36	29.2
1988	38	30.8	29.39	28.17	26.77	127	32.6	31.15	30.25	29.09
1990	35	30.79	29.38	28.16	26.76	158	33.22	31.77	30.24	29.08
1992	32	30.76	29.35	28.13	26.73	151	33.08	31.63	30.21	29.05
1994	58	31	29.59	28.37	26.97	159	33.24	31.79	30.45	29.29
1996	58	31.01	29.6	28.38	26.98	178	33.62	32.17	30.46	29.3
1998	71	31.5	30.09	28.87	27.47	173	33.52	32.07	30.95	29.79
2000	53	31.01	29.6	28.38	26.98	163	33.32	31.87	30.46	29.3
2001	58	31.03	29.62	28.4	27	182	33.7	32.25	30.48	29.32
2002	35	30.83	29.42	28.2	26.8	161	33.68	32.23	30.28	29.12
2003	42	30.87	29.46	28.24	26.84	161	33.66	32.21	30.32	29.16
2004	45	30.94	29.53	28.31	26.91	162	33.3	31.85	30.39	29.23
2005	42	30.86	29.45	28.23	26.83	161	33.28	31.83	30.31	29.15
2006	50	30.96	29.55	28.33	26.93	157	33.2	31.75	30.41	29.25
2007	42	30.92	29.51	28.29	26.89	161	33.18	31.73	30.37	29.21
Avg	54.46	31.10	29.69	28.47	27.07	157.83	33.29	31.84	30.55	29.39
Correlation Coefficient		0.91					0.89			
Diff. Avg. Max/Min Disch. (1968–2007)		103.38 MCM/day								

Source: Prepared by the researcher based on water levels calculated in front of the study stations using the water discharges passing behind Assiut Barrages (Figure 10). Adapted from Sadek, K. A. N. (2010).

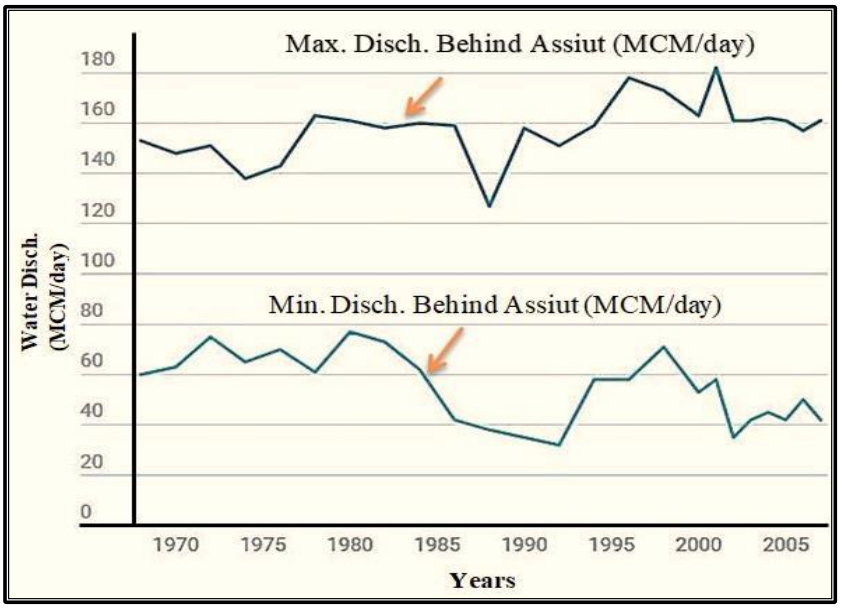

Source: Sadek, K. A. N., 2010, p.81.

Figure 10. Water Discharges Behind Assiut

Barrages During the Period from 1968 to 2007.

Further insights from Table 10, which presents average monthly discharge values behind the Assiut Barrage for the period 1938–2007, demonstrate a distinct seasonal variability in water discharge throughout the year. During the pre-High Dam period (1938–1968), the lowest average discharge occurred in April at approximately 43 (MCM/day), while the highest was recorded in September at 579 (MCM/day). This pattern indicates that the hydrological regime at that time was largely governed by natural seasonal flooding. However, in the post-High Dam period (1995–2007), the extent of seasonal variation in discharge was reduced, with values ranging from 64 (MCM/day) in January to 168 (MCM/day) in June. This change reflects a shift in natural flow patterns due to human intervention in water management and controlled discharge operations. Consequently, it is evident that water discharges downstream of the Assiut Barrage have since become subject to clear annual and seasonal fluctuations, primarily driven by regulatory policies associated with the High Dam's operation. These fluctuations have had a marked impact on the dynamics and stability of the river system.

Table 10. Monthly Average Water Discharges Behind Assiut Barrages during the Period from 1938 to 2007.

Year		Water Discharges Behind Assiut Barrages (MCM/day)											
		Jan	Feb	Mar	Apr	May	Jun	Jul	Aug	Sep	Oct	Nov	Dec
1938-1968		87	66	47	43	86	89	109	440	579	390	166	97
1968-1973		94	88	86	80	98	138	143	130	93	75	76	73
1973-1988		98	80.9	84.9	81.2	94.5	137	146	129	95	81.6	78.9	79.9
1995-2007	Max. Disch	93	108	115	131	153	176	169	160	182	167	147	107
	Avg. Disch	64	77	92	105	130	168	164	150	119	97	92	65
	Min. Disch	30	67	74	87	103	160	151	138	94	67	74	52

Source: Rady (1976) and Sadek & Hekal (2008).

The continuous variation in discharge volumes remains a critical factor affecting bank stability within the study area. Table 10 shows that discharge levels reached their lowest during the months of December and January in the 1995–2007 period, resulting in lowered water levels within the river channel due to the direct relationship between discharge and water

elevation, as illustrated in Table 9. This drop in water level disrupts the hydraulic balance of the banks, intensifying lateral erosion and undercutting processes, thereby increasing the risk of collapse and bank failure. Field observations conducted in January 2025 confirmed these outcomes, with several instances of bank failure observed along the river channel. A particularly illustrative example of this instability is located on the eastern bank of the Nile opposite the village of Beni Samet on the western side. Here, the bank exhibited partial collapses and localized slumping, attributed to undercutting caused by lateral erosion, itself a result of the significant decline in river water levels, as illustrated in Figure 11.

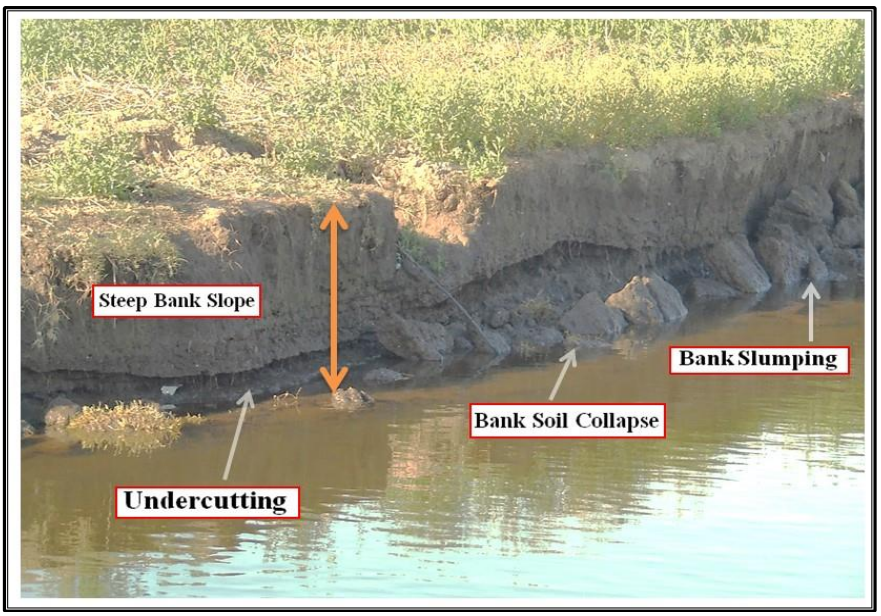

Source: Field Study, 2025.

Figure 11. Exposure of the Eastern River bank Soil of the Nile to Slumping and Partial Collapse West of Beni Samet Village Due to Decreased Water Discharges and the Effect of Lateral Erosion.

6.2. Variations in River Water Levels

The continuous fluctuation in river water levels, resulting from discharge variability within the study area, is one of the principal factors influencing the stability of river banks. Such variations—whether rises or drops—generate two main types of forces acting on the channel banks. The first is internal forces, represented by pore pressure and seepage forces within the porous structure of the bank soil. The second is external forces, commonly referred to as hydrostatic pressure, which is exerted by the water mass on the face of the river bank (Lane & Griffiths, 2000, p. 443). The interaction between these internal and external pressures contributes to weakening bank cohesion and increasing their susceptibility to collapse, particularly during periods marked by repeated and sharp changes in water levels. These instances often coincide with the summer flood season or with winter drawdown periods, such as the winter closure, during which discharge levels are significantly reduced.

Hydrostatic pressures acting on river banks vary in accordance with flow conditions within the channel. When discharges rise, hydrostatic pressure exerted on the bank face increases, which may enhance bank stability depending on the composition and hydro-mechanical properties of the bank materials. In contrast, during abrupt drops in water level, the bank remains saturated for a short period, initially retaining some degree of stability. However, over time, the porous structure of the bank begins to respond, and cohesion weakens as the external hydrostatic support declines. As water levels reach their lowest points, the bank begins to release stored water from its pore structure, allowing it to gradually regain a state of equilibrium and stability once the pressure differential has

dissipated.

This dynamic was confirmed by Ahmed et al. (2010, p. 36), who demonstrated that rapid fluctuations in river water levels—stemming from sharp differences between high and low discharges—accelerate river bank erosion processes and increase their likelihood of collapse. This finding aligns with the conclusions of Schuster and Wieczorek (2018, p. 60), who emphasized that changes in water levels in contact with bank slopes destabilize them and lead to bank failure, particularly in cases of significant or repeated drawdown. Similarly, the study by El-Dien, Takebayashi and Fujita (2014) found that a rapid drop in river water level relative to the time required for pore pressure dissipation within bank soils results in disequilibrium and bank instability. This underscores the necessity of managing water levels in river channels—especially those with cohesive, clay-rich banks—to maintain their structural integrity. The same study also reported that the safety factor for saturated banks when the river channel is filled to the top is approximately 83% of that under dry conditions (El-Dien et al., 2014, p. 48).

Analysis of Table 9 shows marked variations in average water levels associated with annual discharge volumes in the study area, as illustrated in Figure 12. Water levels corresponding to the highest discharges during the 1968–2007 period ranged from 29.39 m to 33.13 m, while those associated with the lowest discharges ranged from 27.07 m to 31.02 m. This variation indicates the direct influence of discharge volume on water levels within the river channel and reflects the dynamic relationship between discharge and stage in the fluvial system. Such discrepancies increase hydrostatic pressure on bank surfaces, which negatively affects their stability, especially during short intervals of alternating high and low discharges.

High water levels during peak discharge periods play a significant role in supporting bank stability by increasing hydrostatic pressure. This helps reduce the pressure differential between internal soil pressure and external water pressure, thereby enhancing cohesion and reducing the risk of failure. This stabilizing effect is most evident during the peak flood season. Data from Table 10 show a clear seasonal variation in the monthly maximum and minimum discharge levels downstream of the Assiut Barrage between 1995 and 2007. Maximum discharges ranged from 93 (MCM/day) in January to 182 (MCM/day) in September, indicating peak flow during the flood months of June to September, which raises water levels in the channel and increases hydraulic pressure on the banks—thus reducing their likelihood of collapse during this period.

Conversely, minimum monthly discharges during the same period ranged from 30 (MCM/day) in January to 160 (MCM/day) in June, a significant gap of 130 (MCM/day). This highlights the sharp decline in discharge during winter months, particularly in December and January, coinciding with the winter closure period (January 7 to February 9), during which water releases are minimized to conserve water for summer irrigation. This sudden drop leads to a significant decrease in channel water levels and, consequently, in the hydrostatic pressure exerted on bank faces. The resultant pressure imbalance weakens bank cohesion and destabilizes them—particularly in steep, clayey banks—making them more susceptible to collapse, especially during periods of sharp and sudden fluctuations in river discharge.

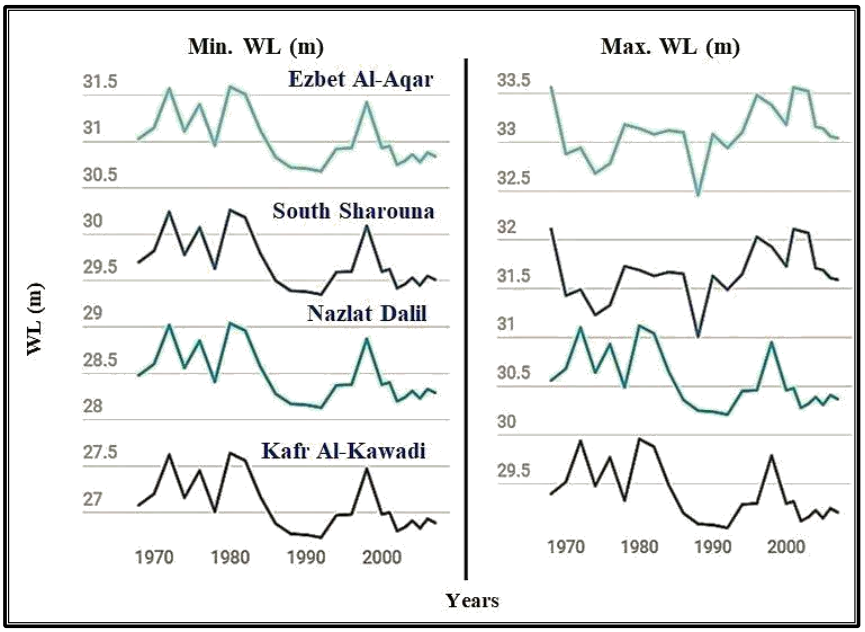

Source: Prepared by the researcher based on data presented in Table 9.

Figure 12. Variations in Nile water levels in the study area during the period 1968–2007 in response to changes in water discharges.

Based on the field study conducted along the banks of the Nile River within the study area in January 2025, five distinct levels of bank erosion were identified on the eastern banks of the river channel, west of the village of El-Sawayta, in accordance with the simulation model presented by McTainsh (1971) (Figure 13), as follows:

- **Level Zero**:

This level refers to the river bank soil that remains submerged under water, lying directly below the lowest observed water level. The soil at this level exhibits relatively stable moisture content, as the hydrostatic pressure exerted by the water contributes to supporting its relative cohesion and stability. This stability contrasts with the higher levels of the bank, which are more susceptible to rapid fluctuations in water levels or partial drying.

- **Level One**:

This level comprises the soil located directly above the minimum water level during high-discharge periods. It remains submerged under such conditions and typically maintains relative stability due to the equilibrium between hydrostatic pressure from the flowing water and the internal moisture content of the soil. However, during low-discharge periods, water levels drop to their minimum, diminishing the stabilizing hydrostatic pressure, which disturbs the equilibrium of the bank and increases the soil's susceptibility to collapse.

- **Level Two**:

This level is situated at a moderate elevation above the channel bed, where water currents begin to gain speed with increasing distance from the shallow bottom. At this elevation, the bank is more exposed to active lateral erosion and undercutting processes. The extent of erosion depends on the composition and cohesion of the bank's soil structure, especially the integrity of its porous matrix. Additionally, erosion is influenced by the combined effect of internal forces (e.g., pore water pressure) and external forces (notably hydrostatic pressure), both of which fluctuate with variations in river discharge.

- **Level Three**:

Located near the upper surface of the river water, this level becomes submerged during high-flow periods. During these times, increased flow velocity and reduced suspended sediment load intensify lateral erosion at this zone. In contrast, during low-flow periods, this part of the bank becomes partially exposed, making it more vulnerable to failure. Repeated erosion at the bank's toe weakens its cohesion, ultimately leading to a loss of balance and bank collapse into

the channel.

- **Level Four**:

This level lies just below the high-water mark reached during peak discharge periods, where water velocities are at their highest. These strong currents intensify lateral erosion processes. The elevated position and steep slope of the bank at this level, combined with the aggressive impact of high-velocity river currents, significantly weaken soil cohesion and disrupt the structural balance of the bank, thereby accelerating failure and collapse.

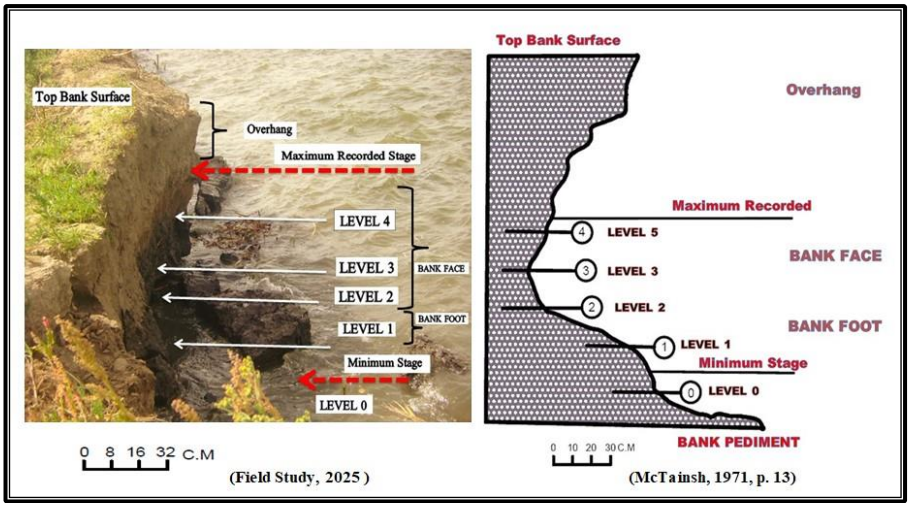

Source: Field Study (2025) and McTainsh (1971).

Figure 13. Longitudinal profile of the eastern river bank west of El-Sawayta village showing the relationship between water level fluctuations and lateral erosion rates along the bank.

6.3. Variability in Flow Velocity

Water currents are defined as the movement of water flowing through the river channel under the influence of gravity. Their velocity within the channel is determined by a combination of hydraulic and geomorphological factors, the most notable of which include water discharge volume, river bed slope, channel depth, bed surface roughness, and sediment load. The study by Roy et al. (1988) indicates a clear positive correlation between flow velocity on one hand, and both channel depth and slope on the other; as depth and slope increase, so too does flow velocity. Conversely, there is an inverse relationship between flow velocity and bed roughness: increased roughness leads to reduced flow velocity due to surface resistance that slows the movement of water and dampens its momentum. Additionally, Yao et al. (2019) highlight the influence of climatic factors on flow velocity during certain times of the year. Wind, for instance, may enhance flow speed when it blows in the same direction as river discharge toward the mouth, as it adds a supplementary driving force to the moving water. On the contrary, when wind opposes the current direction, it slows the flow and introduces turbulence.

Flow velocity is a key factor in determining the intensity and effectiveness of both vertical and lateral erosion processes within a river channel. Increased velocity enhances the river's capacity to erode sedimentary formations along the river bed and banks. This effect becomes particularly pronounced in areas where the river bed is deep adjacent to the bank, creating structural imbalances in the soil and increasing susceptibility to collapse under persistent hydrostatic pressure. The intensity of river bed erosion is governed by two main factors: (1) the eroding force, which is influenced by hydrological and geomorphological variables, primarily discharge volume, channel depth, and longitudinal bed slope; and (2) the erosion velocity, or the critical flow velocity required to initiate the movement of bed sediments of varying sizes from their original positions.

According to H. Salama (2004), the velocity required to initiate erosion increases with decreasing sediment size, due to the high cohesion forces among fine particles such as silt

and clay, which require greater hydraulic energy to overcome. In contrast, coarser sediments—particularly those larger than 0.5 mm—are more easily mobilized at relatively lower flow velocities, which explains the increased efficiency of erosion with larger sediment sizes. This finding aligns with Ibrahim (1981), who confirmed that there is a direct relationship between flow velocity and the particle size of sediments transported by the river. While clay is among the easiest materials to transport due to its low threshold velocity, it is one of the most resistant to erosion due to strong interparticle cohesion. Conversely, sand is more difficult to transport but among the easiest to erode (Ibrahim, 1981, p. 85).

The hydrodynamic characteristics of the Nile River in the study area reveal significant spatial variability in flow velocity across the river's cross-sections, particularly in straight sections devoid of islands. As shown in cross-sections (1, 2, 3) in Table 11, the highest average velocities were recorded in the central part of the channel, ranging from 0.60 m/s to 0.82 m/s. This is attributed to the increased depth in this zone and the reduced influence of lateral friction from the river banks, which enables more streamlined and efficient flow. Moving toward the eastern bank, flow velocity gradually declines, with averages between 0.35 m/s and 0.71 m/s. This reduction is linked to increased friction with the eastern bank and a shallower depth compared to the channel center, which lowers the flow's kinetic energy. The lowest velocities were observed along the western bank, ranging from 0.29 m/s to 0.37 m/s, due to shallower waters and increased friction from both the bed and adjacent bank.

These combined factors intensify lateral erosion on the eastern bank, while promoting sediment deposition along the western bank due to the reduced flow velocity (Figure 14). Additionally, the prevailing north and northwesterly winds—accounting for 48% and 18.2% of occurrences, respectively (Atya, 2019, p. 21)—push surface waters eastward in accordance with Ferrel's Law, thereby enhancing flow speed and stimulating lateral erosion along the eastern bank.

Cross-section (4) in Table 11 shows notable variations in flow dynamics across meander bends. Flow velocity increases on the concave bank, reaching approximately 0.44 m/s. The concentration of flow energy on this side intensifies both vertical and lateral erosion, leading to significant deepening of the channel at this location. This depth disparity causes imbalance in the river bank due to the elevation difference generated by vertical erosion at the base of the bank, often resulting in bank collapse and failure (Figure 15). On the opposite convex bank, flow velocity drops to around 0.31 m/s, due to channel shallowing caused by continuous sediment deposition. This finding is consistent with Obaido (1982), who noted that river depth increases toward the concave side of a bend—where flow velocity and bed scour activity are higher—while decreasing on the convex side due to sediment accumulation (Obaido, 1982, p. 130).

It is also important to note that flow velocity tends to increase along the western banks at the entry and exit points of meander bends (meander wings). This is because the center of curvature in these cases is located on the eastern side, resulting in greater depth and higher erosion rates on the opposite (western) bank due to the increased velocity of water currents. Conversely, deposition occurs on the eastern side, where flow slows down.

Regarding the cross-sectional flow velocity around islands, data from cross-sections (1 and 2) in Table 12 reveal a marked disparity in flow force distribution. Flow velocity increases significantly within the main channel adjacent to the island, ranging from 0.66 m/s to 0.82 m/s, while it decreases in the secondary channel, where it ranges from 0.24 m/s to 0.30 m/s. This difference is attributed to the uneven distribution of discharge between the main and secondary channels, with the main channel receiving the larger share, regardless of whether the island lies within a straight or meandering segment, or whether the main channel is east or west of the island. This indicates that the position of the island relative to the river channel is a decisive factor in determining flow distribution and velocity patterns on either side, independent of the channel's shape or curvature.

Table 11. Horizontal and Vertical Variations in Water Current Velocity across the Nile River Cross-Sections Between Matai and Al-Fashn

Dist. from Aswan Dam (km)	C.S.1 – 723 km (Matai)						C.S.2 – 741 km (Al-Jarabi)					
Meas. Location	Pt. A		Pt. B		Pt. C		Pt. A		Pt. B		Pt. C	
	E (channel)		C (channel)		W (channel)		E (channel)		C (channel)		W (channel)	
	D (m)	V (m/s)	D (m)	V (m/s)	D (m)	V (m/s)	D (m)	V (m/s)	D (m)	V (m/s)	D (m)	V (m/s)
	(m)	(m/s)	(m)	(m/s)	(m)	(m/s)	(m)	(m/s)	(m)	(m/s)	(m)	(m/s)
1	0	1.49	0	1.80	0	0.26	0	0.65	0	0.91	0	0.43
2	0.5	1.51	0.5	1.60	0.5	0.28	0.5	0.39	0.5	0.94	0.5	0.38
3	2.3	1.49	2.3	1.50	1.33	0.69	1.5	0.25	1.5	0.62	1.75	0.21
4	4.6	0.95	4.45	1.18	2.65	0.93	3	0.11	3	0.37	2.7	0.12
5	5.98	0.68	5.79	0.84	3.34	0.40	4	0.00	4.5	0.17	—	—
6	7.1	0.34	8.15	0.65	4.55	0.31	—	—	4.8	0.00	—	—
7	—	—	—	—	—	—	—	—	—	—	—	—
Avg. Velocity (m/s)	0.71		0.82		0.37		0.35		0.60		0.29	
Dist. from Aswan Dam (km)	C.S.3 – 751.8 km (Sharouna)						C.S.4 – 717.5 km (Abu Shehata – Al-Asayat meander)					
Meas. Location	Pt. A		Pt. B		Pt. C		Pt. A		Pt. B		Pt. C	
	E (channel)		C (channel)		W (channel)		E (channel) (Concave Side)		(C .Bank)		E (channel) (Convex Side)	
	D (m)	V (m/s)	D (m)	V (m/s)	D (m)	V (m/s)	D (m)	V (m/s)	D (m)	V (m/s)	D (m)	V (m/s)
	(m)	(m/s)	(m)	(m/s)	(m)	(m/s)	(m)	(m/s)	(m)	(m/s)	(m)	(m/s)
1	0	0.76	0	0.87	0	0.47	0	0.73	0	1.04	0	0.32
2	0.5	0.79	0.5	1.20	0.5	0.49	0.5	0.61	0.5	0.91	0.5	0.36
3	1	0.59	1	0.92	1	0.23	1	0.49	1	0.77	1	0.23
4	2	0.42	2	0.73	1.5	0.18	2	0.24	2	0.61	2	0.15
5	3	0.29	3	0.59	2	0.00	3	0.13	3	0.44	2.3	0.00
6	3.5	0.18	3	0.43	—	—	—	—	3.25	0.32	—	—
7	—	—	4.4	0.21	—	—	—	—	4.5	0.00	—	—
Avg. Velocity (m/s)	0.51		0.71		0.34		0.44		0.68		0.27	

Source: Ministry of Water Resources and Irrigation (MWRI), Nile and Hydraulics Research Institutes. (2007–2008). Unpublished data. Cairo, Egypt.

Table 12. Horizontal and Vertical Variations in Water Current Velocity on Both Sides of River Islands

Dist. from Aswan Dam (km)	C.S.1 – 760 km (Zawiyet AL Gidami Island)				C.S.2 – 767.5 km (Al-Haybah Island)			
Meas. Location	Pt. A		Pt. B		Pt. A		Pt. B	
	Main Channel		Secondary Channel		Secondary Channel		Main Channel	
	E. Zawiyat Al-Gidami Island		W. Zawiyat Al-Gidami Island		E. Al-Haybah Island		W. Al-Haybah Island	
	D (m)	V (m/s)	D (m)	V (m/s)	D (m)	V (m/s)	D (m)	V (m/s)
	(m)	(m/s)	(m)	(m/s)	(m)	(m/s)	(m)	(m/s)
1	0	1.20	0	0.43	0	0.37	0	0.89
2	0.5	0.95	0.5	0.56	0.5	0.43	0.5	0.97
3	2.3	1.20	1.33	0.39	1.7	0.27	1.5	0.88
4	4.6	0.75	2.65	0.24	3.25	0.13	3	0.64
5	5.8	0.54	3.15	0.19	4.2	0.00	4.5	0.39
6	6.5	0.28	4	0.00	—	—	5.25	0.18
Avg. Velocity (m/s)	0.82		0.30		0.24		0.66	

Source: Ministry of Water Resources and Irrigation (MWRI), Nile and Hydraulics Research Institutes. (2007–2008). Unpublished data. Cairo, Egypt.

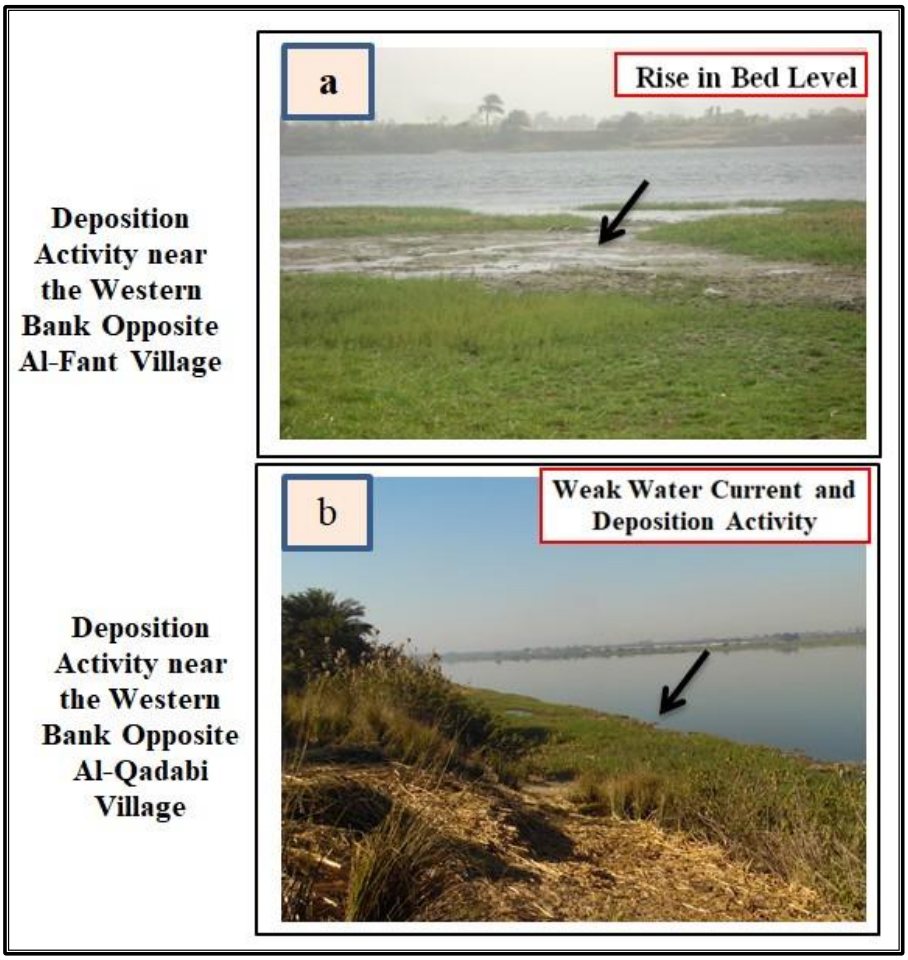

Source: Field Study, 2025.

Figure 14. Deposition activity on the western side of the Nile channel in the study area as a result of reduced water current velocity on the western bank

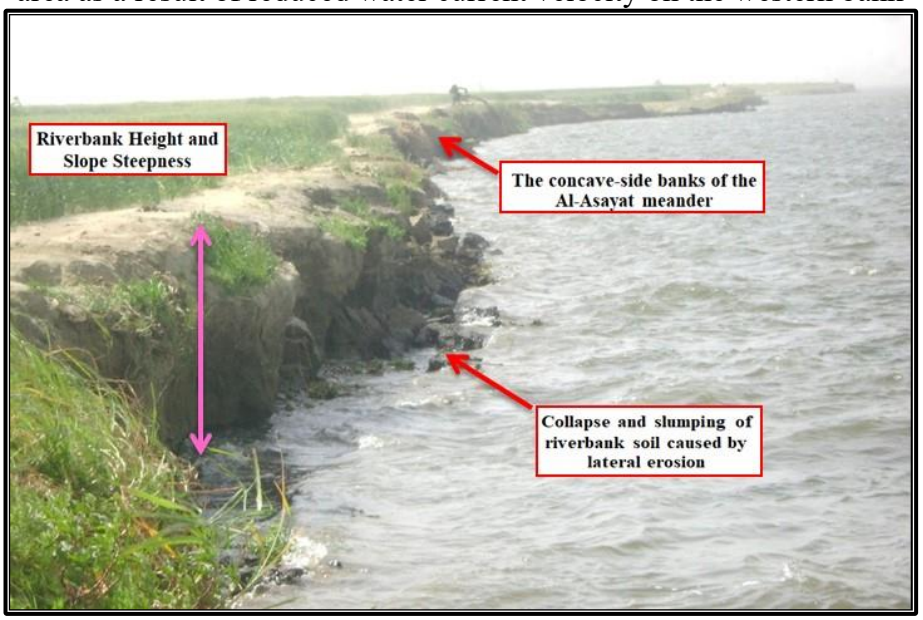

Source: Field Study, 2025.

Figure 15. Collapse and slumping of concave bank soil at Al-Asayat meander due to active vertical and lateral erosion

The results of sediment analysis from Nile River bed samples in the study area, as shown in Table 13, during the period from 1955 to 1958 (prior to the construction of the High Dam), revealed a clear dominance of silty clay sediments and a marked decrease in sand content, which ranged between 18% and 35%, with a complete absence of gravel components in all samples. In contrast, sediment analysis conducted in 2008—approximately 38 years after the High Dam's construction—showed a significant shift in the grain-size composition of bed sediments, with sandy deposits becoming overwhelmingly dominant, accounting for between 97.11% and 99.81%, while clay sediments were entirely absent across all samples. This transformation reflects a change in the sediment dynamics of the channel resulting from hydrological alterations associated with the dam's construction. The sedimentary composition also indicates the predominance of loosely consolidated materials, increasing the bed's susceptibility to flow-induced disturbances, particularly during periods of high discharge. The sandy nature of the deposits plays a critical role in intensifying vertical erosion processes, given their lower resistance to water movement compared to more cohesive clay formations. This risk is magnified when vertical erosion occurs adjacent to river banks, leading to the destabilization of the bank and making it more prone to collapse and slumping—especially in areas with relatively deep channels and an absence of vegetation cover to reinforce the soil.

Moreover, the mechanical analysis of soil samples from the Nile River banks in the study area, as shown in Table 14, reveals a distinct variation in soil composition between the two banks. On the eastern bank, sand content reached an average of 53.4%, while clay accounted for 46.6%. In contrast, the western bank exhibited a higher clay content, averaging 61.8%, with sand declining to 38.2%. This variation is primarily attributed to differences in river flow velocity between the two banks. The eastern bank typically experiences faster currents, enabling the transport and deposition of larger particles such as sand, whereas the reduced flow velocity along the western bank creates favorable conditions for the deposition of finer particles like clay. The elevated sand content on the eastern bank increases its vulnerability to collapse and erosion by fluvial processes, given that sand is less cohesive and more susceptible to disintegration and displacement under the influence of flowing water. As the proportion of sand in the soil increases, its resistance to erosive forces diminishes, accelerating degradation and weakening bank stability (Figure 16 a, b). Conversely, the higher clay content and relative cohesiveness of the western bank reduce erosion and collapse rates, contributing to enhanced soil strength and bank stability (Figure 16 c).

Further mechanical analysis of soil samples from the southern segment of the study area (between river kilometers 705 and 735) also showed notable variations in grain-size composition. On the eastern bank, the average sand content was approximately 62.83%, while clay constituted 37.17%. On the western bank, the sand percentage decreased to 45.97%, whereas clay content increased to 54.03%.

Table 13. Mechanical Analysis of Bed Sediment Samples from the Nile River Channel in the Study Area.

Location	Dist. from Aswan Dam (km)	Description	Gravel (>2)	Coarse Sand (1–0.50)	Medium Sand (0.50–0.25)	Fine Sand (0.25–0.125)	Silt-Clay (<0.0625)	Gravel %	Sand %	Clay %	Total %
			mm								
Before High Dam (1955–1958)											
Behind Assiut Barrage 1955			0	0	0	18	82	0	18	82.0	100
Behind Assiut Barrage 1956			0	0	0	16	84	0	16	84.0	100
Behind Assiut Barrage 1957			0	0	0	34	66	0	34	66.0	100
Behind Assiut Barrage 1958			0	0	0	35	65	0	35	65.0	100
After High Dam (2007–2008)											
El-Sawayta	712.5	E (channel)	1.38	22.57	69.20	6.85	0	1.38	98.62	0	100
		C (channel)	2.68	11.83	74.68	10.81	0	2.68	97.32	0	100
		W (channel)	0.84	4.37	68.83	25.60	0	0.84	98.80	0	100
Kafr El-Sheikh Ibrahim	727	E (channel)	1.35	22.76	66.99	8.90	0	1.35	98.65	0	100
		C (channel)	2.89	12.03	74.24	10.84	0	2.89	97.11	0	100
		W (channel)	0.94	4.63	68.83	25.60	0	0.94	99.06	0	100
Abad Sharouna	752.5	E (channel)	0.19	7.45	72.80	19.56	0	0.19	99.81	0	100
		C (channel)	0.62	11.19	67.05	21.14	0	0.62	99.38	0	100
		W (channel)	0.38	9.07	74.16	16.39	0	0.38	99.62	0	100
Ezbet El-Sa'ayda	760	E (channel)	0.78	16.54	78.76	3.92	0	0.78	99.22	0	100
		C (channel)	0.95	16.26	79.13	3.66	0	0.95	99.05	0	100
		W (channel)	1.28	20.17	75.90	2.65	0	1.28	98.72	0	100

Source: General Nile Control Inspection, unpublished reports (1966–1969); MWRI, Nile Research Institute (NRI) & Hydraulics Research Institute (HRI), unpublished reports (2007–2008).

Table 14. Mechanical Analysis of Bank Soil Sediment Samples from the Nile River Channel in the Study Area.

Dist. from Aswan Dam (km)	Description	Sampling Point (Depth cm)	Gravel (>2)	Very Coarse Sand (2 – 1)	Coarse Sand (1–0.50)	Medium Sand (0.50–0.25)	Fine Sand (0.25–0.125)	Very Fine Sand (0.125 – 0.0625)	Silt-Clay (<0.0625)	Sand %	Clay %	0/0
			(mm)									
705	E. Bank	40	0	3.3	7.60	9.50	18.30	25.10	39.50	60.50	39.50	100
	E. Bank	210	0	9.5	23.30	27.10	8.30	10.70	21.10	78.90	21.10	100
	W. Bank	25	0	1.6	2.10	5.20	14.80	30.27	47.63	52.37	47.63	100
710	E. Bank	65	0	3.4	8.40	7.90	20.30	21.10	40.20	61.10	38.90	100
715	E. Bank	70	0	2.8	5.90	8.70	17.90	22.33	42.37	57.63	42.37	100
	E. Bank	170	0	7.8	17.30	21.60	11.70	12.40	29.20	70.80	29.20	100
721	E. Bank	35	0	1.8	3.90	6.10	12.98	32.75	44.27	55.73	44.27	100
	W. Bank	40	0	0.6	1.40	7.90	19.12	21.87	49.71	50.29	49.71	100
734	E. Bank	45	0	1.1	2.10	8.10	9.83	31.75	48.22	51.78	48.22	100
	W. Bank	30	0	0	2.90	4.40	14.87	24.23	53.60	46.40	53.60	100
735	E. Bank	45	0	0.8	3.70	5.30	7.94	27.30	55.76	44.24	55.76	100
	E. Bank	190	0	3.4	14.30	27.60	18.70	21.40	14.60	85.40	14.60	100
	W. Bank	40	0	0	1.20	4.78	11.34	17.50	65.18	34.82	65.18	100
740	E. Bank	50	0	0	0	4.55	9.30	26.52	59.63	40.37	59.63	100
	W. Bank	40	0	0	0	3.60	12.77	14.93	68.70	31.30	68.70	100
750	E. Bank	65	0	0	2.10	6.70	13.40	19.90	57.90	42.10	57.90	100
752	E. Bank	50	0	0	0.00	4.80	7.30	23.00	64.90	35.10	64.90	100
760	E. Bank	65	0	0	0	4.55	9.30	26.52	59.63	40.37	59.63	100
	E. Bank	210	0	0	11.80	23.10	26.10	33.40	5.60	94.40	5.60	100
	W. Bank	35	0	0	0	5.90	11.20	12.20	70.70	29.30	70.70	100
762	E. Bank	80	0	0	2	3.90	8.90	28.12	56.78	43.22	56.78	100
	W. Bank	55	0	0	0	4.70	9.70	11.60	74.00	26.00	74.00	100
770	E. Bank	35	0	0	0	2.80	10.90	21.90	64.40	35.60	64.40	100
	E. Bank	180	0	0	10.30	17.20	33.70	35.20	3.60	96.40	3.60	100
	W. Bank	40	0	0	0	1.25	7.30	14.93	76.52	23.48	76.52	100

Source: Prepared by the researcher based on the field study (2025); analysis conducted at the Geography Department Laboratory, Faculty of Arts, Benha University.

In contrast, soil samples collected from the river banks in the northern part of the study area, between kilometers 735 and 770, revealed a clear shift in sedimentary characteristics. The average sand content on the eastern bank was approximately 53.44%, while clay accounted for 46.56%. On the western bank, the average sand content declined further to just 26.72%, whereas clay content increased to 73.28%. This sedimentary pattern serves as a distinct geomorphological indicator of transformations within the fluvial system, particularly in relation to the dynamics of river flow and its direct impact on soil properties and bank stability. The gradation in sediment characteristics along the Nile's banks in the study area is attributed to the marked variation in flow velocity, both between the two banks and along the river's course from south to north. Higher flow velocity along the eastern bank promotes the transport and deposition of coarser sediments such as sand, while reduced velocity near the western bank leads to the deposition of finer particles like silt and clay. This sediment distribution has a direct effect on bank stability: the eastern bank, with its high sand content, is less cohesive and thus more prone to collapse and slumping. In contrast, the relatively cohesive clay-rich soils on the western bank contribute to increased structural integrity and resistance to erosion, thereby enhancing the overall stability of the river banks.

Source: Field Study, 2025.

Figure 16. Variation in erosion rates on both river banks due to differences in bank soil composition

6.4. Decline in Fluvial Sediment Load

Suspended load is a fundamental component in maintaining the natural equilibrium within the fluvial system, as it regulates the relationship between flow energy on the one hand, and the nature of the river bed and banks on the other. Any disruption to this balance—particularly in the form of reduced suspended and bed load volumes—results in the release of surplus energy within the water flow, which in turn intensifies vertical and lateral erosion processes. Consequently, reduced sediment supply leads to channel deepening, bank undercutting, and the destabilization of river banks, especially in locations where soils are composed of weakly cohesive materials. Data from Table 15 indicates a significant decline in the annual volume of suspended load in the Nile River between 1955 and 1973. In 1950, the annual load was approximately 134.4 (M Tons/Year), reflecting the volume of sediment transported by natural flooding prior to the construction of the High Dam. However, with the commencement of the High Dam project, this volume began to decrease steadily, reaching only 4.4 (M Tons/Year) per year by 1970—a decline of over 130 (M Tons/Year) per year (Figure 17). This dramatic reduction is attributed to the

entrapment of enormous quantities of silt in Lake Nasser behind the dam, which effectively severed the natural sediment supply to the downstream river channel. The decline continued in subsequent years, with annual suspended loads dropping below 4 (M Tons/Year), disrupting the sedimentary balance of the river system and increasing its latent erosive energy. This shift contributed to intensified vertical and lateral erosion, resulting in channel deepening and the deterioration of bank stability. Table 15 also reveals a sharp decline in annual averages of bed load after the construction of the High Dam, reflecting the broader reduction in transported sediment. Bed load dropped from approximately 13.1 (M Tons/Year) per year in 1964 to just 0.4 (M Tons/Year) in 1977—a difference of 12.7 million tons per year—due to the severe decrease in sediment supply following the dam's construction. This reduction enhanced the river's erosive power, particularly in combination with the slower subsurface currents near the river bed (Table 11), which allowed for continued scouring and deepening of the channel. Furthermore, the increased sand content in bed sediments (Table 13) facilitated this erosion, even under conditions of reduced suspended load, which previously contributed significantly to vertical erosion through its additional scouring force. I. Salama (2004), attributed the reduced velocity of bottom currents to the role of subsurface flows in carrying fragmented bed sediments and employing them as tools for deepening the channel, thereby slowing the near-bed flow. Meanwhile, H. Salama (2004), noted that suspended sediment concentration is highest near the river bed and decreases toward the surface, which in turn reduces the flow velocity close to the channel bottom.

Table 15. Total Suspended Sediment Load in the Nile Water Behind Assiut Barrages during the Period from 1955 to 1973

Year	Avg. Annual Suspended Load (M tons/yr)	Avg. Annual Bed Load (M tons/yr)
1955	134.428	—
1960	103.9	—
1961	111.0	—
1962	105.0	—
1963	96.7	—
1964	38.7	13.1
1965	16.5	2.2
1966	9.0	2.7
1967	14.4	5.2
1968	3.2	0.3
1969	3.7	0.4
1970	4.4	0.5
1971	4.5	0.5
1972	4.8	0.5
1973	4.5	0.4
1974	4.2	0.3
1975	3.30	0.4
1976	3.05	0.4
1977	3.10	0.4
Load Diff. (M tons/yr)	131.3	12.7

Source: Ministry of Irrigation (1966, 1971); Rady (1976); Ministry of Water Resources and Irrigation (2003).

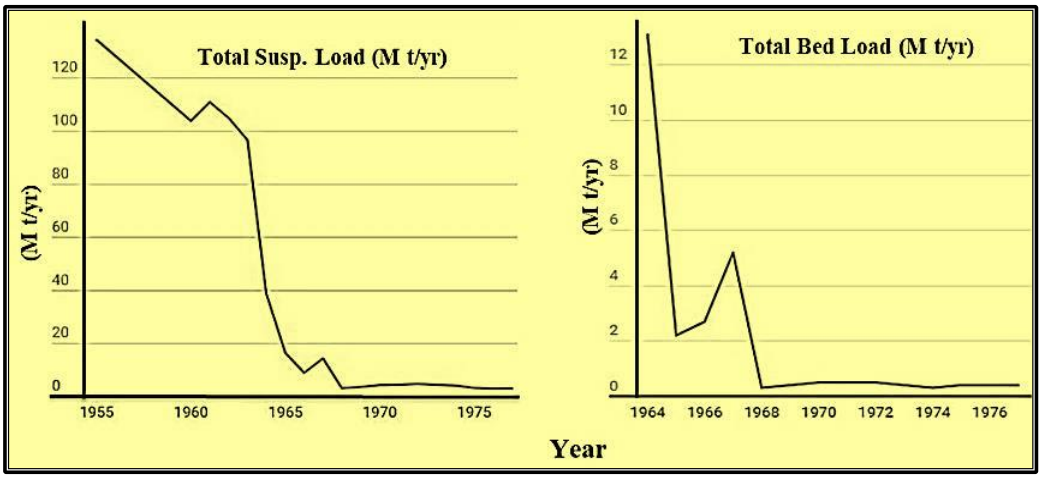

Source: Prepared by the researcher based on Table 9.

Figure 17. Sharp decline in average suspended and bed load annually behind Assiut Barrages after the construction of the High Dam.

6.5. Riparian Soil Moisture

Soil moisture is considered one of the most critical natural factors directly influencing the behavior and mechanical properties of soil, particularly in terms of its cohesion, structural stability, and susceptibility to erosion and slippage under hydrological and climatic influences. In this context, moisture refers to the amount of water retained between soil particles, whether in the form of capillary water or water bound to soil molecules. This directly affects the internal forces that either enhance soil cohesion or lead to its disintegration. The soil's response to moisture varies depending on its type and texture. Sandy soils, characterized by large particles and wide pores, allow water to infiltrate rapidly and retain little of it, leading to a significant reduction in internal friction and rendering the soil unstable when saturated. Conversely, clay soils, composed of fine particles with high water retention capacity, tend to exhibit relatively strong cohesion under moderate moisture levels, yet become prone to slippage or collapse under full saturation or sudden moisture fluctuations.

Understanding the relationship between soil properties and moisture behavior is therefore a foundational aspect in analyzing the dynamics of riparian bank stability within the study area and in interpreting the banks' susceptibility to collapse or resistance under variable river discharge and changing climatic conditions. Mechanical analysis results of soil samples from the eastern banks of the Nile River reveal a clear variation in sand and clay content (Table 14), indicating sedimentological differences with direct implications for the soil's hydro-mechanical properties and bank stability. Sand content in the study samples ranged between 23.5% and 96.4%, highlighting the heterogeneity of the eastern bank soils. Three primary soil types can be distinguished based on structural composition and moisture response (Table 16):

- **Type I:** Soils with sand content exceeding 80%. These are classified as coarse-grained sandy soils (2.0 – 0.063 mm) and are structurally loose, lacking cohesive forces. Their mechanical behavior relies solely on internal friction, which is significantly reduced upon saturation, resulting in high vulnerability to collapse and landslides—especially under cyclonic rainfall or elevated river water levels. The typical moisture content for these soils ranges between (25–30%), with negligible cohesion due to the absence of fine components such as clay and silt. These soils exhibit no identifiable plastic or liquid limits.
- **Type II:** Mixed riparian soils with sand content ranging between 40% and 60%. These fall under the Sandy Clay category, with particle sizes between (0.50 – 0.002 mm). They demonstrate relatively better cohesion due to the presence of clay particles, which improve moisture resistance. At moderate moisture levels (20–30%), these soils exhibit

cohesive forces ranging between (20–35 kPa), contributing to relative bank stability. However, prolonged moisture exposure or surpassing the liquid limit (LL = 30–40%) leads to disintegration of the internal structure, increasing the likelihood of surface sliding or gradual cracking and instability.

- **Type III:** Clay-dominant riparian soils with sand content below 40%, indicating the prevalence of clays such as Illite or Montmorillonite. These soils, at moderate moisture levels (25–35%), demonstrate relatively high cohesion (25–60 kPa), offering substantial structural stability. Nevertheless, they are sensitive to excessive moisture. When the liquid limit is exceeded—ranging from 50–60% for Illite and up to 90–100% for Montmorillonite—the soil structure degrades, turning into a soft, low-resistance medium. This poses significant risks, especially along steep river banks or areas subjected to recurrent hydrological pressure due to discharge fluctuations or cyclonic rainfall.

Table 16. Comparative Analysis of Moisture Behavior and Cohesion Types in Sandy and Clay Soils and Their Impact on Fluvial Stability

Soil Type	Dominant Moisture Type	Typical Moisture Content (%)	Liquid Limit (LL)	Cohesion (kPa)	Dominant Grain Size Range (mm)	Effect of Moisture on Overall Stability	Relation to Bank Stability
Sandy Soil	Free moisture – does not create cohesion and increases collapse risk when saturated. Free moisture is among the most hazardous types for soil stability, especially in sandy areas, as it does not contribute to cohesion and its increase due to rainfall or rising discharge leads to instability and structural collapse.	**25–30% (at saturation)**	**Not applicable**	**≈ 0**	**2.00 – 0.063**	**Internal friction sharply decreases upon saturation, leading to loss of cohesion and increased collapse**	Riverbanks are highly prone to sliding and collapse, especially after rainfall, high discharge, or under ongoing fluvial erosion
Sandy Clay	Capillary moisture + partial intergranular moisture	**20–25%**	**LL ≈ 30–40%**	**10–25 kPa**	**0.50 – 0.002**	**Moderate cohesion at medium moisture, gradually decreases as moisture increases**	Riverbanks show relative stability under unsaturated conditions due to moderate structural cohesion, but become prone to failure and sliding when LL is exceeded due to sudden saturation, leading to weakening and disintegration under gravity or surface runoff
Clayey Loam	(Capillary moisture + partially adsorbed moisture). Moisture exists as capillary water between fine pores and partially bound water on particle surfaces, both contributing to structural cohesion in semi-saturated clayey soils.	**20–30%**	**LL ≈ 30–40%**	**20–35 kPa**	**0.05 – 0.002**	**Shows good cohesion at moderate moisture, weakens with increasing moisture**	This type is prone to gradual structural-level slips due to the wet softening effect, where continuous moisture increase reduces internal cohesion, especially in upper layers, weakening structural integrity and causing slow slips or creeping cracks in steep or water-pressured banks
Clay (Kaolinite, Illite)	(Partially bound moisture + capillary water between clay plates). The soil retains partially adsorbed moisture and capillary water trapped between clay layers, contributing to its relative cohesion under unsaturated conditions.	**25–35%**	**LL: 30–60%**	**25–60 kPa**	**< 0.002 mm**	**Maintains cohesion under moderate moisture, collapses gradually when LL is exceeded**	Shows relative stability under moderate moisture; however, sustained water pressure or sudden water level changes reduce structural cohesion, increasing risk of slow surface slips or partial collapses, especially in steep or highly porous banks
Montmorillonite Clay	(Capillary moisture + tightly bound water + high swelling potential). This soil has capillary water in fine pores and strongly bound water on particle surfaces, allowing high moisture retention and strong expansion when saturated, directly impacting its structure and stability.	**30–40% and up to 60%**	**LL: 90–100%**	**Up to 60 kPa (pre-saturation)**	**< 0.002 mm (very fine)**	**Partially cohesive, but collapses significantly under full saturation or sudden drying**	Apparent stability only; extremely hazardous with fluctuating water levels or periodic drying/flooding, leading to rapid deformation and collapse

Source: Adapted and synthesized from multiple references on soil mechanics and hydromechanical behavior, including: Gillott (1968), Grim (1968), Lambe & Whitman (1969), Fredlund & Rahardjo (1993), Moore & Reynolds (1997), Craig (2004), Lu & Likos (2004), Mitchell & Soga (2005), Murray (2007), Rahardjo et al. (2007), Holtz et al. (2011), Das (2013), and Dezső et al. (2019).

This classification reveals that the stability of the eastern banks of the Nile River is directly linked to soil type, particle-size distribution, and the soil's response to moisture. Loose sandy soils, characterized by high sand content and low cohesive strength, are the most vulnerable to slippage and collapse, particularly under full saturation conditions. This is due to the reduction in internal friction and the absence of active clay minerals. In contrast, mixed soils (sandy clays) exhibit relative stability at moderate moisture levels, but remain susceptible to structural disintegration once the liquid limit is exceeded. Clay-rich soils containing minerals such as illite or montmorillonite, while displaying higher cohesion, are highly sensitive to elevated

moisture levels, which can lead to gradual softening and structural deformation under prolonged saturation or sudden fluctuations in water levels. Therefore, risk factors are not solely dependent on sand or clay percentages, but also on the type of clay present, liquid limit thresholds, and actual moisture content in the soil.

Mechanical analysis of soil samples from the western river banks indicates a relative dominance of clay content over sand (Table 14), suggesting a markedly different depositional pattern compared to the eastern banks. Clay content in the western samples ranged from 47.6% to 76.5%, reflecting a more cohesive structural composition, which significantly influences soil-moisture interaction and bank stability. Based on sedimentary composition and hydromechanical behavior, the western river bank soils can be classified into three main types according to their structural makeup and moisture response (Table 16):

- **Type I:** Soils with clay content exceeding 70%, such as samples from Zawiyat al-Gidami, Ezbet al-‘Aqar, and Ezbet al-Sa‘ayda. Dominant particle sizes in these soils range from <0.002 mm to 0.062 mm, representing fine clay and silt. These soils are typically composed of pure clay—predominantly illitic or kaolinitic. At moderate moisture levels (20–30%), they display relatively high cohesive strength (5–60 kPa), providing good structural stability. However, when moisture exceeds the liquid limit (LL = 30–60%), the soil structure begins to deteriorate, transforming into a weak, plastic medium. This increases the potential for structural failure, particularly in steeply sloped banks or those exposed to repeated hydrological stress from cyclonic rainfall or fluctuating river levels.
- **Type II:** Soils with clay content between 60% and 70%, generally classified as clayey loam, often exhibiting characteristics of kaolinitic clay. These soils are composed of a blend of fine clay (<0.002 mm), silt, and fine sand (0.062–0.25 mm), resulting in a transitional structure between sandy and clayey soils. At moderate moisture levels (20–30%), these soils demonstrate good cohesion (20–35 kPa), offering reasonable resistance to slippage. However, prolonged saturation or surpassing the liquid limit (LL = 30–40%) progressively weakens the soil structure, increasing the likelihood of slow surface sliding or shallow cracking.
- **Type III:** Mixed soils with clay content ranging from 45% to 60%, classified as silty clay to sandy clay. These soils encompass a broader range of particle sizes, including fine clay and silt (<0.062 mm) combined with fine to medium sand (0.125–0.5 mm). Typically dominated by kaolinitic or illitic clays, these soils exhibit a balanced combination of cohesion and flexibility. At moderate moisture content (25–30%), they display strong cohesive forces (25–60 kPa), making them more resistant to structural failure than the other two types. Nonetheless, when the moisture level exceeds the liquid limit (LL = 30–60%), the soil gradually loses cohesion and becomes increasingly susceptible to slippage and collapse—particularly on steep slopes or in areas under recurrent hydrological pressure due to cyclonic rainfall or rising river levels.

From the above, it is evident that the western bank tends toward fine-textured clay-rich soils with a high proportion of particles smaller than 0.062 mm, granting them relatively high structural cohesion under dry or moderately moist conditions (20–30%). This behavior is attributed to the dominance of kaolinitic and illitic clays, which confer cohesive forces ranging from 25 to 60 kPa, maintaining relative stability as long as moisture levels remain below the liquid limit (30–60%). However, this stability is not guaranteed over time. Prolonged saturation—such as rising water tables or continuous moisture seepage—can progressively reduce cohesion, leading to surface cracks or slope failure in steeply inclined banks. Therefore, understanding the interplay between grain size distribution, moisture levels, and cohesive limits is fundamental for geomorphological assessment of river bank failure risks along the Nile River. This underscores the need for regular monitoring of soil moisture and hydrological activity in these areas.

7. Spatial Assessment of River bank Hazard Levels Between Matai and Al-Fashn Based on Their Hydromechanical Properties and Hydrological Changes Affecting Bank Soil Stability

River banks are among the most sensitive components of the fluvial system to environmental changes, as they are continuously influenced by a complex interplay of factors that include the hydrological characteristics of river flow on one hand, and the structural and mechanical properties of the bank soils on the other. These combined factors play a critical role in determining the stability of river banks or their susceptibility to erosion and collapse, particularly in light of the major hydrological transformations that have occurred in the Nile River following the construction of the High Dam. This part of the study is significant for its aim to analyze and assess the spatial patterns of hazard levels along the river banks by correlating the hydromechanical properties of the soil—such as moisture type, cohesion forces, and liquid limit—with influential hydrological variables, including fluctuations in discharge and water level. This integrative approach enabled the classification of river banks into varying degrees of risk (from low to high), depending on their responsiveness to these hydromechanical influences.

7.1. First Classification: Determining Hazard Levels Based on the Hydromechanical Properties of Soil

Hazard levels were classified based on composite indicators that represent the interaction between the physical and mechanical properties of the soil and the influencing hydrological factors, as detailed in Table 17. These indicators include the percentages of sand and clay, dominant moisture type, cohesion level, approximate liquid limit, and the prevailing grain size distribution. This classification reflects the pivotal role of the soil's hydromechanical characteristics in determining its hazard potential. High sand content, when accompanied by low cohesion and the presence of free moisture, tends to increase the hazard level. Conversely, cohesive clay-rich soils enhance structural stability and resistance to collapse. The analysis revealed clear spatial variation between the two banks and along the south–north gradient, owing to differing sedimentary and hydrological conditions.

7.1.1. Eastern Bank:

- **Southern Sector (705–734 km): High-Hazard Soils**

Soils in this sector are characterized by a high sand content (58.6%) relative to clay (41.4%), resulting in silty sand with a relatively coarse grain structure (fine sand–silt), as shown in Table 17. This soil is classified as "high-hazard" due to its weak cohesion and rapid water saturation, which lead to reduced structural resistance and heightened susceptibility to failure, particularly during high discharge events or abrupt fluctuations in water level.

- **Middle Sector (734–752 km): Medium-Hazard Soils**

In this sector, the soils tend toward silty clay, with a clay content of approximately (54.5%) and sand at 45.5%, featuring a fine grain structure (silt–very fine sand). The soil demonstrates medium cohesion (15–25 kPa) according to Table 17, providing it with a moderate degree of structural resistance. However, prolonged moisture exposure and full saturation compromise its structural integrity. Thus, this sector is classified as "medium-hazard," due to the soil's sensitivity to moisture and water level variability, which could lead to cohesion loss under unstable hydrological conditions.

- **Northern Sector (752–775 km): Medium to High-Hazard Soils**

Here, the clay content rises to (60.7%), while sand decreases to (39.3%), producing sandy clay soil with medium to high cohesion (25–40 kPa), as shown in Table 17. Although the high clay content enhances soil stability, the presence of fine sand increases its susceptibility to gradual cohesion loss under surface flow or sudden water level changes. This justifies its classification as "medium to high hazard," as its structural integrity is closely tied to the surrounding hydrological stability.

Table 17. Classification of Hazard Levels Along the River Nile Banks Between Matai and Al-Fashn Based on Soil Hydromechanical Properties

Bank Side	Sector (km from Aswan)	Dominant Soil Type	Sand Content (%)	Clay Content (%)	Dominant Grain Size	Estimated Cohesion (kPa)	Predominant Moisture Type	Approx. Liquid Limit (LL%)	General Hazard Level	Reason for Classification
Eastern Bank	Southern Sector 705–734	Sandy loam	58.6	41.4	Fine sand – silt (0.25–0.0625 mm)	Weak (≈ 5–15)	Free moisture / Capillary	Not defined (likely low)	High	Sandy bank soil, weak in cohesion, prone to loss of strength under saturation. Rapid collapse may occur when water levels rise due to high discharge rates.
	Middle Sector Sector 734–752	Silty clay	45.5	54.5	Very fine sand – silt	Moderate (15–25)	Capillary moisture	LL ~ 30–40%	Moderate	Bank soil with higher cohesion, though it remains vulnerable to structural degradation when reaching full water saturation.
	Northern Sector 752–775	Clayey sandy soil	39.3	60.7	Silt – very fine sand	Moderate to high (25–40)	Capillary and adsorbed	LL ~ 40–60%	Moderate–High	Bank soil with high clay content, relatively stable, but the granular structure makes it prone to disintegration under runoff or sudden water level changes.
Western Bank	Southern Sector 705–734	Loamy sand	49.7	50.3	Fine sand – silt (0.25–0.0625 mm)	Weak (≈ 10)	Free moisture	Undefined / low	High	Mixed bank soil, with moderate cohesion, but affected by high moisture. Partially vulnerable to erosion on slopes; increased sand content reduces cohesion under runoff or water level rise caused by high discharges.
	Middle Sector Sector 734–752	Clay soil (silty clay)	33.1	66.9	Clay + silt (0.0625–0.002 mm)	Moderate to high (25–45)	Capillary	LL ~ 40–50%	Low	Highly cohesive clayey bank soil, resistant to erosion and collapse except under prolonged saturation or if banks are steep.
	Northern Sector 752–775	Pure clay (kaolinitic/illitic)	26.3	74	Fine clay < 0.002 mm	High (45–60)	Adsorbed / capillary moisture	LL > 50%	Very Low	Highly cohesive soil, strongly resistant to erosion and degradation, stable under most hydrological conditions.

Source: The hazard classification table for the River Nile banks between Matai and Al-Fashn was developed by the researcher, based on the analysis and interpretation of data presented in Tables 14 and 16.

7.1.2. Western Bank:

- **Southern Sector (705–734 km): High-Hazard Soils**

Soils in this sector exhibit near-equal proportions of sand (49.7%) and clay (50.3%), resulting in sandy silty soil with relatively balanced grain composition. However, the low cohesion (approximately 10 kPa) and the presence of free, unbound moisture significantly weaken the soil's mechanical resistance—especially along slopes or during periods of high water levels. Consequently, these river banks are classified as "high hazard" (Table 17) due to their structural instability under fluctuating hydrological conditions.

- **Middle Sector (734–752 km): Low-Hazard Soils**

In this sector, the clay content reaches 66.9%, while the sand content drops to (33.1%), forming fine-grained soil (silt and clay) with medium to high cohesion (25–45 kPa). Capillary moisture predominates, which enhances the soil's structural stability and provides good resistance to erosion and collapse—except under prolonged saturation or in steeply sloped areas. Based on these characteristics, this portion of the river bank is classified as "low hazard" (Table 17) and is considered the most stable zone on the western bank (Figure 18).

- **Northern Sector (752–775 km): Very Low-Hazard Soils**

This sector contains the highest clay content recorded in the study area (74.0%) and the lowest sand proportion (26.3%). The soil is characterized by an extremely fine-grained, clayey (pelitic) structure (<0.002 mm), with high cohesion (45–60 kPa) and a high liquid limit (>50%). These properties confer strong resistance to various hydrological impacts, including erosion and collapse, even during prolonged saturation periods. As a result, these river banks are classified as "very low hazard" (Table 17; Figure 18), given their high structural cohesion and marked stability under varying hydrological conditions.

The results of the first classification clearly

demonstrate that the stability of the river banks in the study area is strongly influenced by spatial variability in the hydromechanical properties of the soil—particularly clay content, dominant moisture type, and liquid limit. The eastern bank appears more vulnerable to hazard (Figure 18), especially in its southern sector, due to the predominance of low-cohesion sandy soils that saturate quickly and thus increase the likelihood of structural failure and collapse under fluctuating water levels. In contrast, the western bank exhibits relatively greater stability, particularly in the northern sector, where high clay content, elevated cohesion, and high liquid limits contribute to increased resistance against erosion and sediment displacement. Moreover, a spatial gradient in hazard levels is evident from south to north on both banks, although the intensity and nature of this gradient vary. Analytical indicators suggest that the most significant factors promoting river bank stability include high clay content, the presence of capillary or absorbed moisture, and elevated cohesion. Conversely, the highest hazard levels are associated with sandy soils characterized by low cohesion and the presence of free water content.

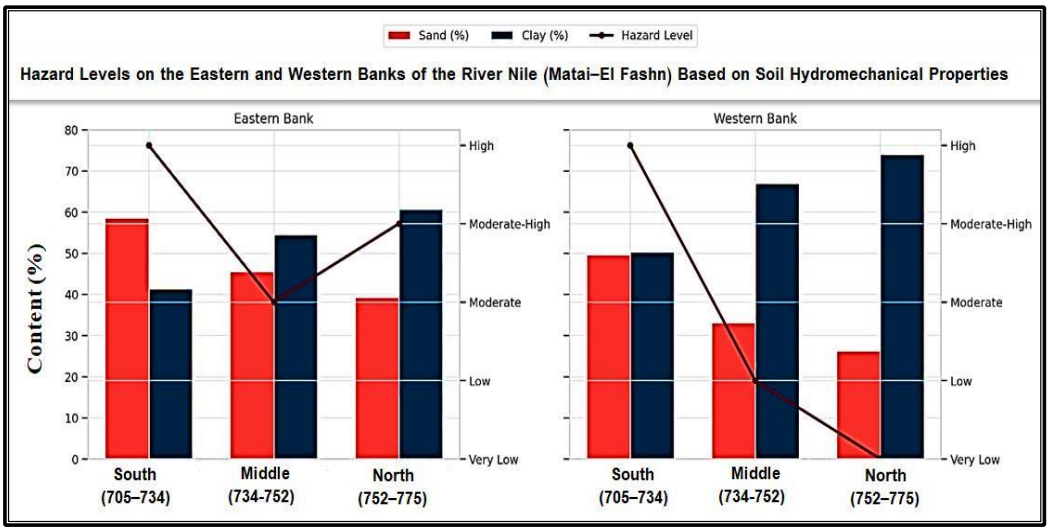

Source: Prepared by the researcher based on Table 17.

Figure 18. Hazard Levels on the Eastern and Western Banks of the River Nile (Matai–El Fashn) Based on Soil Hydromechanical Properties

7.2. Second Classification: Assessing River bank Hazard Levels Based on the Interaction Between Hydromechanical Soil Properties and Channel Depth Under Hydrological Fluctuations

This classification integrates the physical and mechanical properties of bank soils (such as clay and sand content, cohesion, and liquid limit) with channel characteristics—particularly average bed depth—to evaluate the river banks' response to sudden or seasonal variations in water discharge and levels. Channel depth plays a critical role in determining the type and duration of hydraulic pressure exerted on the banks: deeper channels prolong the effect and buffer sharp fluctuations, whereas shallower channels accelerate the transfer of hydraulic pressure to the banks, causing direct erosion or surface collapse.

The study revealed a complex interaction between soil type and bed depth that directly affects bank stability under high or low flow conditions. Loose, sandy soils with low cohesion are more susceptible to collapse during high discharge, particularly in shallow channels. In contrast, cohesive clay-rich soils demonstrate greater stability, especially when coupled with deeper channels that mitigate the impact of hydrological changes. Accordingly, the Nile River banks between Al-Fashn and Matai were classified into three hazard levels under this framework, based on grain composition, moisture type, cohesion level, bed depth, and bank behavior during hydrological fluctuations (Table 18).

- **Southern Sector (705–734 km): High-Risk River banks**

The river banks in this sector exhibit hydromechanical properties that make them among the most prone to collapse within the study area. The bank soils are composed of sandy silty and loamy sand textures, with high sand content (49.7–58.6%) and moderate clay content (41.4–50.3%), resulting in a loosely structured matrix with low cohesion (5–15 kPa). This composition renders the soil vulnerable to sudden internal structural changes, especially in the presence of free or capillary moisture, which accelerates saturation and structural weakening, thereby reducing its resistance to shear stress—particularly during abrupt shifts in water levels.

The average channel depth is approximately 4.98 m, a relatively shallow depth that makes the banks more sensitive to hydrological fluctuations. During periods of high discharge, the hydrostatic pressure of the water may offer temporary lateral support to the banks, reducing the likelihood of collapse. However, the greatest risk arises when discharge levels drop suddenly, removing this hydraulic support and leaving saturated banks exposed to undercutting by lateral erosion and abrupt collapse—especially along steep or unvegetated slopes.

During low-flow periods, the bank soils tend to lose moisture and experience shrinkage, leading to the formation of structural clay cracks. This weakening of soil structure reduces cohesion and increases the likelihood of surface slippage or gradual subsidence along the banks (Figure 19). Thus, the combination of loose sandy texture, low cohesion, presence of free water, and limited channel depth produces hydromechanical conditions that significantly heighten the susceptibility of this sector's banks to collapse under hydrological variation, particularly during sudden drops in discharge. This justifies their classification as a high-risk zone (Table 18; Figure 20).

Table 18. Hazard Classification of the Nile River Banks (Matai–Al-Fashn) Based on Channel Depth and Hydromechanical Soil Properties under Hydrological Fluctuations.

Study Area	Sector (km from Aswan)	Dominant Soil Type	Sand (%)	Clay (%)	Cohesion (kPa)	Dominant Moisture Type	Liquid Limit (LL%)	Average Bed Elevation (m)	Risk under High Discharge	Risk under Low Discharge	General Hazard Level	Reason for Classification
Matai – El-Fashn	Southern Sector 705–734	Sandy loam + Loamy sand	49.7 – 58.6	41.4 – 50.3	Low (5–15)	Free / Capillary moisture	Not identified (Low)	4.98	Temporary hydrostatic pressure may support the banks briefly, but sudden discharge drop causes rapid saturation and failure.	Partial drying leads to structural cracking, weakening the soil cohesion and triggering gradual subsidence or shallow sliding.	High	Sandy soil with weak cohesion; saturates quickly under high discharge, increasing collapse risk. The shallow bed depth intensifies vertical seepage and stress on the bank base.
	Central Sector 734–752	Silty clay + Clay soil	33.1 – 45.5	54.5 – 66.9	Moderate to high (15–45)	Capillary moisture	30–50%	5.02	Shows moderate resistance; hydrostatic pressure at medium depth provides partial support, but basal scour may occur in steep or exposed sections.	Gradual moisture accumulation creates negative pore pressure that weakens the lower layers, especially under repeated wet-dry cycles.	Moderate – Low	Soil is more cohesive, yet internal water suction during discharge fluctuation can reduce stability, particularly in steep slopes or areas with weak vegetation cover.
	Northern Sector 752–775	Clayey sandy + Pure clay	26.3 – 39.3	60.7 – 74.0	Very high (25–60)	Capillary / Adsorbed	40–60% → >50%	6.19	Deep hydrostatic pressure stabilizes the bank base and prevents erosive forces from penetrating; surface effects under high discharge are negligible.	Soil structure remains stable; minor impact from low discharge occurs only in rare cases like prolonged saturation or extreme slopes.	Very Low	Highly cohesive, fine-grained clay soil; the deep riverbed increases hydrostatic pressure and reinforces bank resistance—making this sector a model of natural stability.

Source: The hazard classification table for the River Nile banks between Matai and Al-Fashn was developed by the researcher, based on the analysis and interpretation of data presented in Tables 4 and 14.

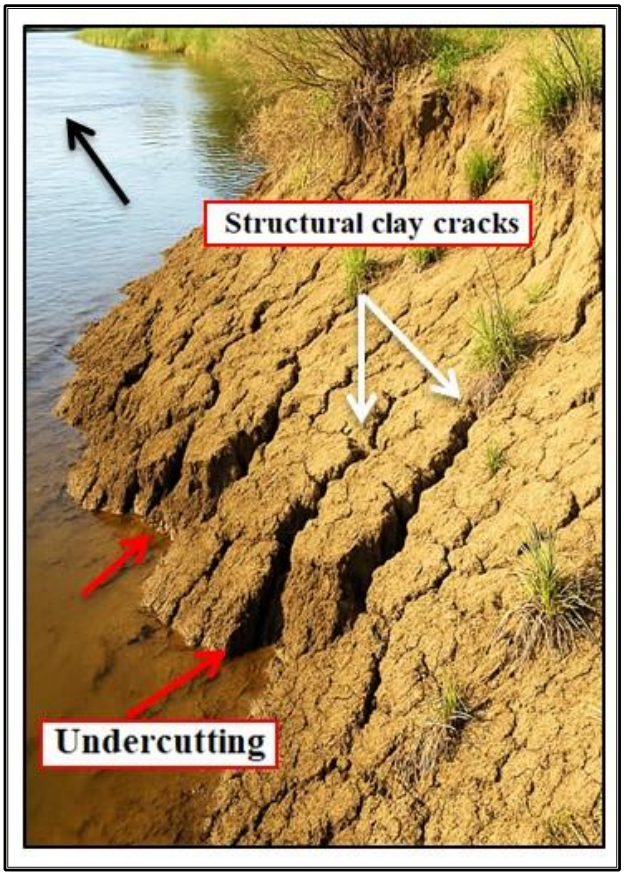

Source: Field Study, 2025.

Figure 19. Cracks in river bank soil resulting from decreased water discharge and moisture loss, which led to reduced soil cohesion and active basal undercutting of the banks *(Eastern bank – South of Sheikh Hassan)*

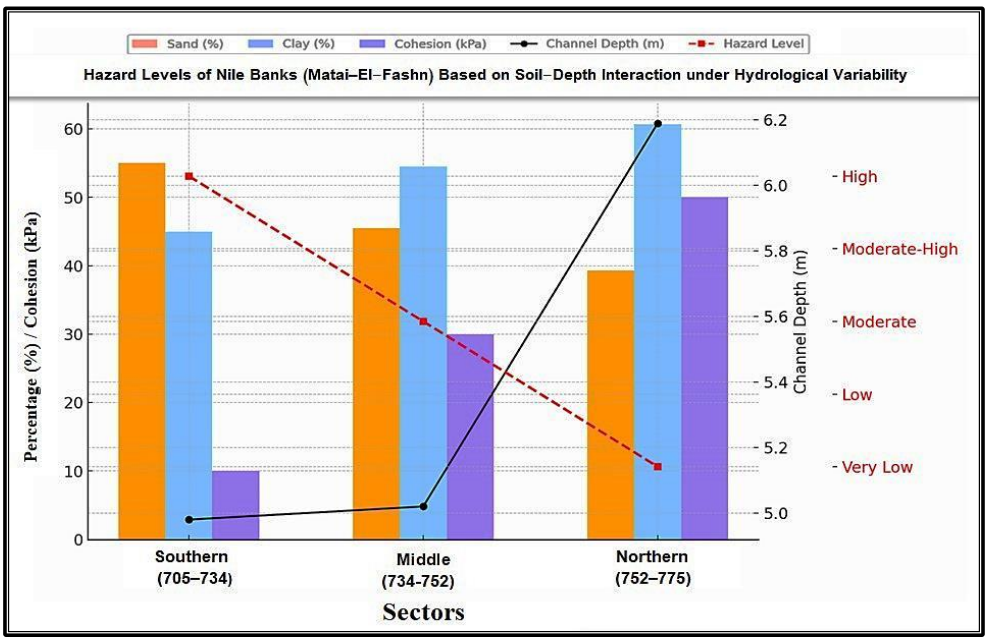

Source: Prepared by the researcher based on Table 18.

Figure 20. Hazard Levels of the Nile River Banks (Matai–Al-Fashn) Based on Channel Depth and the Hydromechanical Properties of Bank Soils under the Influence of Discharge Fluctuations

- **Middle Sector (734–752 km): Moderate to Low Risk River banks**

The bank soils in this sector exhibit more cohesive hydromechanical characteristics compared to those in the southern sector. They primarily consist of silty clay and pure clay soils, with a relatively high clay content ranging between 54.5% and 66.9%, and a lower sand content between 33.1% and 45.5%. This composition provides greater structural stability under hydrological changes due to the fine-grained texture, which offers strong resistance to riverine erosion and collapse. Soil cohesion values in this area range from (15 to 45 kPa), indicating moderate to high internal bonding between particles, which contributes to delaying slope failure even under sudden changes in water discharge.

Capillary moisture is the dominant form of water present in these soils. Unlike free moisture, capillary water aids in stabilizing the soil structure without inducing full saturation, thereby helping to maintain relatively stable river bank conditions under normal flow regimes. The average river bed depth in this sector is about 5.02 m—a transitional depth that is neither shallow nor deep—resulting in a variable influence of water level fluctuations on bank stability, depending on slope gradient and the presence of protective vegetation.

During periods of high discharge, hydrostatic pressure provides temporary lateral support to the river banks, which reduces the likelihood of sudden collapse. However, limited undercutting may occur at steep bank sections. When discharge decreases, the reduction in water pressure—while moisture remains trapped within the soil—can lead to the development of negative pore pressure, which gradually weakens the lower layers of the bank soils. If wetting and drying cycles repeat over time, this dynamic interaction may trigger slow surface slips or subsidence along the river bank, particularly in areas with fragile soil textures, steep gradients, or poor vegetative cover.

Based on these conditions, the river banks in this sector are classified as moderate to low risk (Table 18; Figure 20), due to the relative balance between adequate cohesion levels, stable moisture content, and moderate channel depth. Nonetheless, sustained hydraulic pressures or recurring hydrological fluctuations could compromise the stability of certain structurally weak zones, especially those with steep slopes or insufficient vegetation (Figure 21).

Source: Field Study, 2025.

Figure 21. Gradual Weakening and Structural Failure of Riverbank Soil due to Discharge Reduction and Repeated Wetting–Drying Cycles (North of Bani Samet).

- **Northern Sector (752–775 km) – Very Low Risk River banks**

The bank soils in this section exhibit the highest levels of structural and hydro-mechanical stability across the entire study area, owing to their fine structural characteristics and exceptional capacity to maintain cohesion under hydraulic pressure and discharge fluctuations. The soil consists of a clay-rich mixture comprising pure clay and clayey sandy textures, with a very high clay content (60.7% and 74.0%) and a comparatively low sand fraction (26.3%–39.3%). The bank soils here possess an extremely fine microstructure (less than 0.002 mm), which contributes to enhancing their internal cohesion, ranging between (25 and 60 kPa). This endows the banks with high mechanical resistance to shear forces and erosion, even under sudden hydrological fluctuations. The soil moisture regime is dominated by capillary and adsorbed water—two of the most stable forms of soil moisture—which do not cause immediate saturation but help maintain structural cohesion without inducing rapid changes in the soil's physical properties. From a hydrological standpoint, the average bed level in this section is approximately 6.19 m, the highest among all sections. This considerable depth is a key factor, as it provides stable hydrostatic pressure that prevents forceful river water infiltration into the bank soils, thereby protecting the internal layers from scouring and collapse. During high-discharge periods, this pressure reduces undercutting rates and maintains the banks in mechanical equilibrium, while also mitigating the effects of sudden fluctuations in water levels. Under low-discharge conditions or during prolonged saturation, the clay soils demonstrate a high capacity to retain their structural integrity (Figure 22), due to their small particle size and strong molecular bonding. This provides effective resistance against collapse and creep forces. Consequently, the likelihood of structural failures or subsidence remains very low, occurring only under exceptional circumstances such as steep slopes or areas of inherent structural weakness. Accordingly, this section is classified as a very low-risk zone, based on the balanced interaction between the highly cohesive clay composition of the bank soils, the stability of their moisture content, and the presence of a deep channel that enhances the stabilizing effect of hydrostatic pressure—all of which contribute to increasing the banks' resistance to collapse and erosion resulting from hydrological fluctuations.

Source: Field Study, 2025.

Figure 22. Retention of Structural Cohesion in Clayey River bank Soil during Low Discharge due to Fine Particle Size and Strong Molecular Bonding (Eastern Bank – West of Al-Aqr Village)

The results of the second classification showed that the variation in risk levels along the Nile River banks within the study area is closely related to the interactive relationship between river bank soil properties (particularly clay content, cohesion, and moisture type) and the depth of the adjacent channel. It was found that river banks composed of loose sandy soils with low cohesion and free water content, especially in shallow channels, exhibit the highest hazard rates, as in the southern sector. In contrast, the northern sectors showed high stability due to the high clay content, fine structure, elevated cohesion, and greater channel depth that generates stabilizing hydrostatic pressure on the banks. The data also showed a gradual decrease in hazard levels from south (high risk) to north (very low risk) (Table 18, Figure 20), with differences in response patterns between the eastern and western banks. Analytical indicators suggest that the key factors contributing to river bank stability include increased clay content, high soil cohesion, capillary or adsorbed moisture, and channel depth, while the highest hazard levels are associated with loosely structured, low-cohesion soils with free water content and rapid saturation under variable discharge conditions.

8. Preventive and Reinforcement Measures for the Protection of River bank Soils

River banks represent highly sensitive zones within any fluvial system, as their stability is influenced by a complex interaction between the structural properties of the soil and the hydrological factors associated with discharge and water level fluctuations. The results of the hydromechanical classification of the Nile River banks within the study area revealed that hazard levels are not solely determined by the physical composition of the soil, but are also affected by its degree of saturation, the prevailing moisture type, cohesion and liquid limit values, as well as by the depth of the channel and its response to discharge variations. In this context, effective river bank protection requires a tailored approach that adapts preventive and reinforcement measures to the dominant soil type on each bank, while taking into account its behavior under hydrodynamic forces. For instance, sandy soils exhibit heightened sensitivity to rapid water currents due to their low cohesion and high saturation rate, whereas clayey soils possess greater resistance but may be subject to internal pore pressure that weakens structural cohesion under sudden hydraulic loading caused by discharge fluctuations. Accordingly, this section of the study offers a practical framework aimed at classifying the necessary engineering, environmental, and regulatory interventions for river bank protection, based on the type of soil and its hydromechanical characteristics. It is also grounded in a thorough analysis of soil behavior under both high and low discharge conditions and provides specialized technical recommendations to establish long-term structural stability of the river banks.

8.1. Protection of River banks with Sandy Soils

Sandy river bank soils require a combination of preventive and engineering measures to ensure their stability under the influence of fluctuating discharge and water level variations. Riprap lining with large stones is considered an effective solution for protecting river banks against lateral erosion (Figure 23a), as the rock masses serve to dissipate the energy of water currents and prevent soil erosion, particularly in areas exposed to strong or recurrent flows. Studies have shown that reducing the bank slope angle to approximately 26.6° contributes to minimizing the risk of collapse, especially in weakly cohesive sandy soils (Environmental Planning & Design, LLC, 2021). Additionally, gabion structures—wire mesh baskets filled with stones—are used to reinforce steep river banks (Figure 23b), as they help stabilize the soil and mitigate erosion by distributing loads and preventing lateral slippage (Bhandari, 2019). Another supportive measure involves slope regrading by reducing the slope angle to a safe level not exceeding 30°, preferably between 26° and 28° in cases of frequent saturation or weakly cohesive sandy soils, in order to minimize shear forces and enhance the overall stability of the bank. Bioengineering methods further support this stability through the planting of vegetation with strong root systems, such as common reed (*Phragmites australis*), turf

grasses, and small species of *Halfa* (Figure 23c), in addition to eucalyptus and willow trees. These plants contribute to surface stability by anchoring the soil and increasing its resistance to erosion, and they are well-adapted to alternating wet and dry conditions, which is particularly important in sandy environments where moisture is rapidly lost. Therefore, stabilizing sandy river banks requires the implementation of integrated solutions that take into account the weak granular structure of these soils and aim to reduce the impact of hydraulic forces while enhancing the soil's ability to withstand erosion and collapse in both the short and long term.

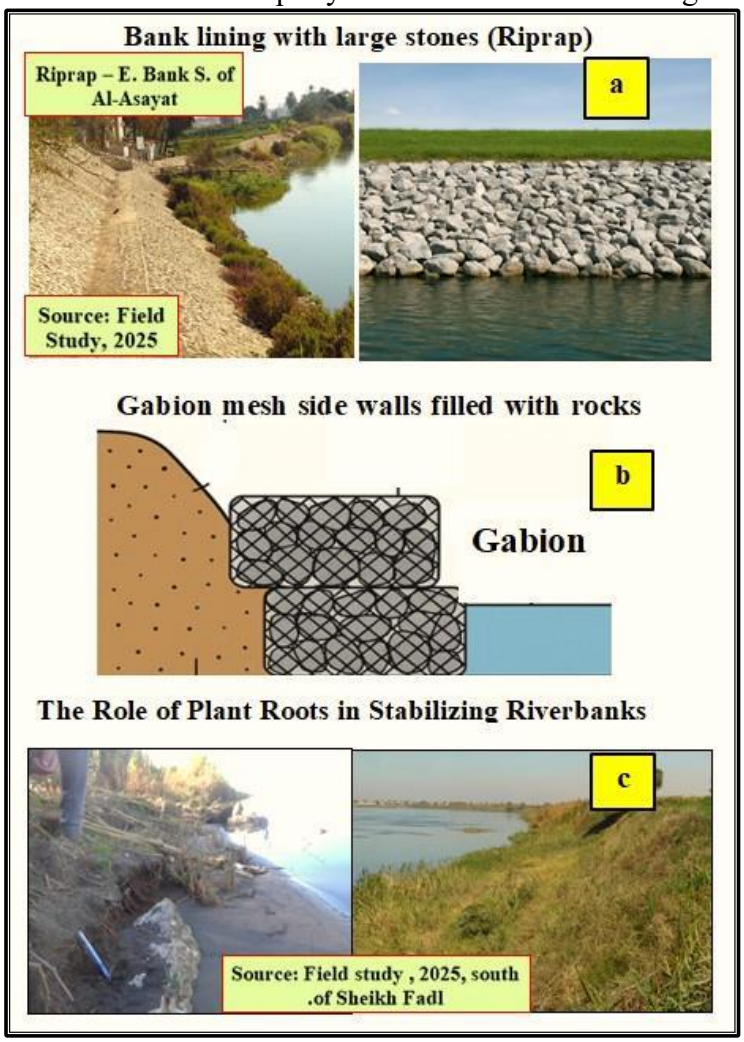

Source: The illustrative figures were generated for research purposes using artificial intelligence (OpenAI, 2025), and Field Study, 2025.

Figure 23. Engineering and Bio-technical Solutions to Enhance the Stability of Sandy River banks.

8.2. Protection of River banks with Sandy Clay / Clayey Sand Soils

Sandy clay and clayey sand soils represent a transitional state in terms of structure and hydromechanical properties, falling between sandy and clayey soils. To enhance the stability of river banks composed of this soil type, it is recommended to adopt a dual protection strategy that combines moderate structural reinforcement with improved natural drainage and resistance capacity of the soil. From an engineering perspective, the use of sloped backfills covered with geotextile fabrics (geotextile-lined revetments) is considered an effective method (Figure 24a), as these fabrics help stabilize the soil and prevent the loss of fine particles due to water movement, thereby reducing erosion rates at the base of the bank (Koerner, 2012). Additionally, semi-permeable barriers (permeable barriers) offer supportive protection (Figure 24b), as they help slow down water flow

near the river banks and gradually distribute hydraulic pressure, thus mitigating the impacts of lateral erosion and sudden pressure fluctuations (Prasad, Indulekha, & Balan, 2016). From a biological standpoint, it is preferable to use plants with moderately deep root systems that do not induce structural cracks upon soil drying, such as certain native tree species adapted to fluctuating moisture levels, including eucalyptus, mulberry (*Morus alba*), *Ziziphus spina-christi* (sidr), and common reed (*Phragmites australis*), the latter being commonly used by local inhabitants in the study area as a traditional method for stabilizing sandy clay soils (Figure 25). The vegetative cover should be balanced and not overly dense, allowing for adequate soil aeration while preventing excessive moisture retention.

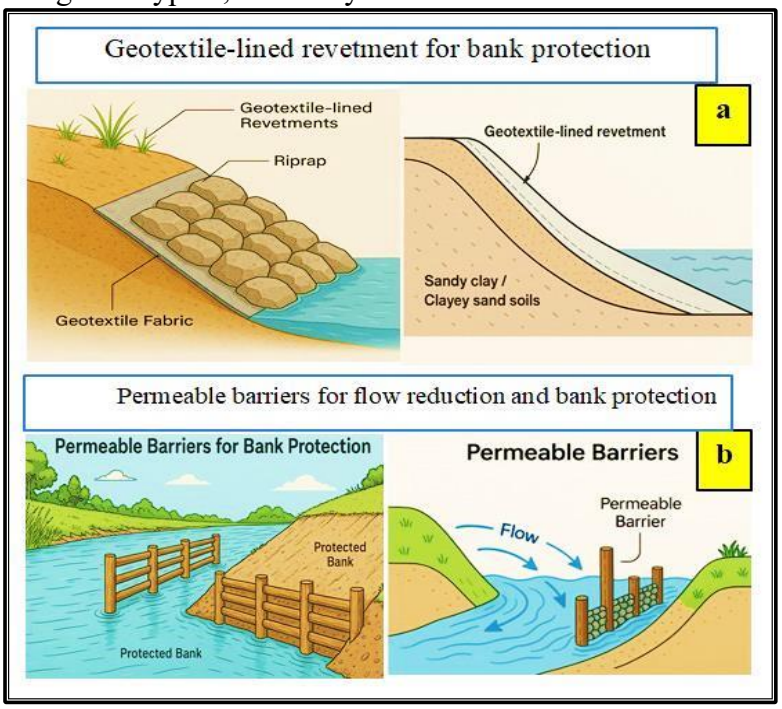

Source: The illustrative figures were generated for research purposes using artificial intelligence (OpenAI, 2025).

Figure 24. Engineering Solutions to Enhance the Stability of Sandy-Clay River banks

Source: Field Study, 2025.

Figure 25. Farmers plant dense vegetation on sandy-clay river banks to improve soil cohesion and contribute to bank stability

8.3. Protection of River banks with Clay Soils

Clay river banks are among the most sensitive environments to hydrological changes and mechanical stresses due to their fine-grained structure and rapid response to saturation and drying, which makes them susceptible to cracking and structural failure—particularly under fluctuating water levels or ongoing erosion processes. Protecting such banks requires integrated strategies that account for the physical characteristics of the soil and its behavior under hydraulic stress conditions. Recent studies recommend an approach that combines geotechnical reinforcement and hydraulic control, alongside enhancing natural stability through vegetative cover.

Deep injection techniques using low-concentration cementitious materials or biodegradable polymers have proven effective in improving soil resistance to shear stress and cracking while maintaining permeability. However, their application is often limited by high costs, specialized equipment, and the need for precise execution, making large-scale implementation challenging. Consequently, vegetative solutions present a more sustainable and cost-effective alternative. Indigenous deep-rooted species—such as *Phragmites australis* (common reed) and *Acacia nilotica* (Nile acacia)—can significantly improve soil cohesion and reduce erosion. These natural measures can be reinforced through regulatory interventions aimed at controlling discharge levels, thereby maintaining stable pore water pressures and minimizing the adverse impacts of water level fluctuations, particularly during seasonal low-flow periods.

In addition, lightweight hydraulic structures—such as submerged vanes or guide vanes—can be installed to reduce flow velocity near the banks, especially along concave meanders. These should be designed in alignment with the specific characteristics of the river reach, ensuring they do not disrupt ecological or hydrological balance. Such structures help deflect flow away from erosion-prone banks, reducing direct hydraulic stress and promoting the deposition of fine sediments near the river bed, which in turn strengthens the bank base and enhances overall structural stability. The use of rigid concrete structures is generally discouraged in these fragile environments, except in extreme cases where necessary; and even then, design and implementation must consider the geotechnical properties of the soil—such as shear strength, liquid limit, and plasticity index—to ensure long-term structural safety and stability.

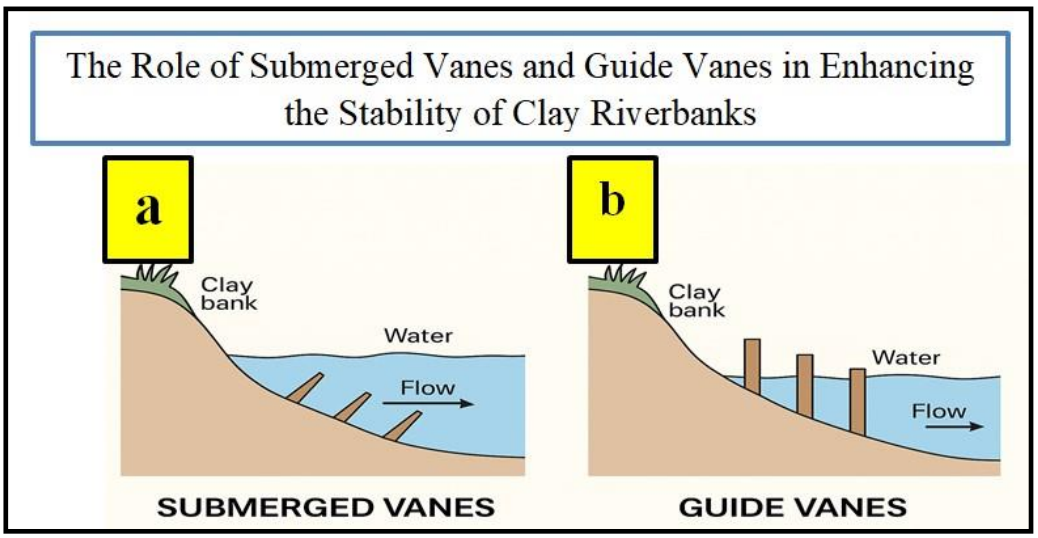

Source: The illustrative figures were generated for research purposes using artificial intelligence (OpenAI, 2025).

Figure 26. Hydro-mechanical Protection Techniques for Clay River banks Using Submerged and Guide Vanes

8.4. Community and Technological Monitoring as Pillars of River bank Stability

- Legal and Regulatory Measures are essential for reducing anthropogenic pressures on river
- banks. This includes establishing a legally defined river buffer zone where construction, agriculture, and dredging are prohibited, setting clear land-use regulations for areas adjacent to the river, and enforcing penalties for practices that compromise the structural stability of the banks.
- Technological Monitoring relies on Remote Sensing (RS) and Geographic Information Systems (GIS) to observe morphological transformations along river banks and to analyze changes in channel shape or bank retreat. These tools enable early intervention before risks escalate.
- Community-Based and Planning Strategies play a complementary role in ensuring the sustainability of protection measures. This involves raising local awareness about the ecological and structural significance of river banks, highlighting the risks associated with certain agricultural and urban activities near bank edges, and encouraging community participation in routine maintenance campaigns, vegetation belt planting, and reporting violations within the protected river buffer zone. It is also recommended to prepare updated hazard maps, redirect urban and agricultural development away from high-risk areas, rehabilitate degraded river banks, and restore ecological balance along the river course.

9. Results

- The Nile River channel between Matai and Al-Fashn has undergone gradual and profound morphological transformations over the past seven decades, reflected in increased sinuosity and length, and reduced width and water surface area. These changes result from the complex interaction between hydrological factors and river bank soil characteristics, along with the cumulative impacts of human interventions—particularly following the construction of the High Dam—which have disrupted the river's natural equilibrium and intensified lateral erosion rates, compromising bank stability.
- The study demonstrates that river islands and meanders now serve as vital indicators of fluvial system disturbance, rather than mere byproducts of erosion or deposition. The evolving patterns of these morphological units reflect the river's reactive behavior to new conditions: islands signify the hydraulic dynamics of water currents, while meanders represent structural stress points along the flow path. Consequently, analyzing their characteristics is no longer solely a topographic concern, but a necessity for assessing bank stability and understanding channel behavior over time.
- The findings confirm that the morphological changes in the Nile's channel are not solely the result of natural processes, but stem from the joint interaction of hydrological dynamics and anthropogenic activities. Reduced water discharge and suspended sediment loads have contributed to selective sedimentation along the western bank and increased lateral erosion on the eastern bank. This has disrupted the balance between banks and introduced a spatial bias in river bank dynamics. Human interventions—such as infilling secondary channels—have transformed certain islands into floodplain extensions, causing internal morphological alterations like reduced water surface area and disrupted channel linearity.
- The Nile is currently trending toward lateral expansion and abandonment of secondary channels, aligning with its diminished energy and reduced longitudinal development capacity. This behavior indicates a state of "unstable equilibrium," in which limited morphological changes occur without reaching a fully stable condition. Therefore, continuous monitoring of channel behavior, particularly in areas showing signs of bank weakening or failure, is critically needed.
- The results show that the transformation of the Nile's hydrological regime after the High Dam's construction triggered a fundamental shift in channel dynamics, affecting both flow behavior and the physical properties of bank-

forming soils, leading to diminished bank stability. The wide fluctuations in discharge—both annually and seasonally—have caused hydraulic imbalances along the banks, especially during periods of sharp decline, thereby increasing lateral erosion and undercutting at the bank bases, particularly on the eastern side of the channel.

- The study confirms that repeated water level fluctuations exert a dual influence on bank stability through pore pressure within the soil and hydrostatic stress caused by changes in water levels at the bank interface. This continuous variation weakens soil cohesion, especially during the winter closure period or abrupt water level drops, increasing the risk of sliding in clay soils and collapse in sandy banks.
- The significant reduction in suspended sediment following the dam's construction has disrupted the river's sediment balance. The absence of clay input has freed additional stream energy, intensifying vertical erosion of the channel bed, deepening the channel, and weakening banks—particularly in areas with sandy or structurally loose soils.
- The study reveals that channel depth is a decisive factor in how banks respond to hydrological changes. Deep channels act as hydraulic buffers, reducing the transmission of sudden pressure to the banks and providing temporary support and relative stability. In contrast, shallow channels facilitate rapid hydraulic pressure transfer, weakening soil and increasing the likelihood of erosion and collapse, especially during sudden water level drops.
- The mechanical analysis of bank soils indicates that grain composition is a key determinant of structural bank stability. Sandy soils, despite containing moderate moisture levels, exhibit significant weakness upon saturation. Conversely, clay soils—especially those rich in illite or kaolinite minerals—display relatively high cohesion under dry conditions but lose much of it progressively under continuous saturation or abrupt water level changes.
- The initial hazard classification results show that hydromechanical soil properties are critical in determining river bank hazard levels. Banks composed mainly of sandy or sandy silt soils with low cohesion and high free moisture show high susceptibility to structural collapse, particularly in southern sections. In contrast, banks dominated by fine clay soils with higher cohesion and capillary or absorbed moisture exhibit greater structural stability, especially in northern sectors.
- The second hazard classification underscores that the interaction between soil characteristics and channel depth adds an additional dimension to understanding bank stability. Findings reveal that banks with loosely packed sandy soils and shallow channels are most vulnerable to erosion and collapse due to the rapid transmission of hydraulic pressure to the bank base. Meanwhile, banks composed of deep clay soils show greater resilience, even under fluctuating hydrological conditions.
- The spatial assessment of river bank characteristics reveals a clear gradient of hazard levels from south to north on both sides of the Nile. The highest hazard levels are recorded in the southern sector, where structurally weak sandy soils dominate. In contrast, hazard levels decrease progressively northward, where cohesive fine clay soils with greater hydraulic resistance prevail.
- The study concludes that relying solely on engineering solutions is insufficient for achieving effective and long-term river bank protection without the implementation of integrated environmental, legislative, and community-based strategies that account for soil variability. Bio-interventions, such as bioengineering and the use of vegetation tailored to soil types, are effective in enhancing bank stability, especially in moderately cohesive areas. These solutions gain importance due to their ability to reduce dependence on rigid structures while offering flexible and sustainable protection. Their effectiveness, however, depends on selecting plant species appropriate for each soil type, integrating them with suitable agricultural

practices, slope regrading, and flow regulation. These measures must be supported by precise monitoring systems and expanded community engagement in observing changes and maintaining bank stability.

10. Recommendations

- Adoption of an integrated monitoring system for morphological and hydrological changes affecting the river channel, by activating a periodic surveillance framework based on remote sensing technologies and Geographic Information Systems (GIS) to track changes in the Nile River's course and its islands. These changes should be regarded as early warning signs of potential instability along the river banks, which could lead to future erosion or collapse. This can be achieved through the use of aerial photographs and satellite imagery, verified by field visits to confirm changes on the ground.
- Activation of regular technical monitoring systems for river banks using Remote Sensing (RS) and GIS technologies, in order to detect morphological transformations and early stages of bank erosion. This approach enables the implementation of preventive measures based on up-to-date dynamic data and allows timely interventions before risks escalate.
- The necessity of adopting an integrated assessment approach to analyze river bank stability, combining soil properties (such as sand and clay content, cohesion levels, and moisture type) with channel characteristics (such as bed depth and discharge behavior), to ensure a comprehensive understanding of risk nature and to accurately identify weak zones.
- Adoption of a more flexible and balanced water management policy that minimizes abrupt fluctuations in water discharge, particularly during the winter closure period or seasonal transitions, due to their direct impact on water level variations and hydrostatic pressure reduction—both of which are key contributing factors to the collapse of weak clay and sandy banks.
- Inclusion of hazard classification, based on the interaction between soil characteristics and channel depth, as a planning tool in river management. This classification should serve as a design reference for any protective engineering works or economic exploitation of lands adjacent to the river channel.
- Classification of river bank soils into stability units based on their grain composition and moisture response patterns, accompanied by the assignment of appropriate engineering reinforcement programs for each type to mitigate soil slips and collapses along the river banks.
- Reevaluation of the impact of human interventions on the river channel from a long-term cumulative perspective, rather than as isolated localized events. The study highlights that encroachments and infilling of secondary channels have cumulative effects on flow behavior and hydraulic energy distribution. It recommends the imposition of strict land-use regulations on both sides of the river within a clearly defined corridor subject to legislative oversight, to reduce direct pressures on the main bank—particularly around meanders and in front of river islands that cause localized flow disturbances.
- Preservation of natural vegetation cover along the river banks, especially in areas with steep slopes, due to its important role in reinforcing soil cohesion and reducing the impact of erosion.
- Strengthening the role of local communities in river bank protection through awareness campaigns and active participation in afforestation efforts, maintenance activities, and reporting of encroachments. This participatory approach enhances the actual sustainability of protective measures.

11. Sources and References

11.1. Sources

Egyptian General Petroleum Corporation (EGPC), & Conoco Coral. (1987). *Geological Map of Beni Suef (NH 36 SW), Scale 1:500,000*. EGPC.

Egyptian General Survey Authority. (1991). *Topographic Maps, Scale 1:50,000* (3 Sheets). Egyptian General Survey Authority.

Egyptian Survey Authority. (1953). *Topographic*

Maps, Scale 1:25,000 (5 sheets). Egyptian Survey Authority.

Environmental Planning & Design, LLC. (2021, June 15). *Pittsburgh River Bank Mapping and Prioritization Final Report*. City of Pittsburgh. https://apps.pittsburghpa.gov/redtail/images/16664_Pittsburgh_Riverbank_Mapping_Final_Report_15JUN2021.pdf

Ministry of Irrigation – General Nile Control Inspectorate. (1966). *Potential Erosion Studies of the Nile River Channel Downstream of the High Dam – Report No. 1*. Ministry of Irrigation.

Ministry of Irrigation – General Nile Control Inspectorate. (1971). *Potential erosion Studies of the Nile River Channel Downstream of the High Dam*. Ministry of Irrigation.

Ministry of Water Resources and Irrigation – Nile River Protection and Development Sector. (2003). *Nile River Channel Protection and Development Project: Annual technical report*. National Water Research Center, Nile Research Institute.

Ministry of Water Resources and Irrigation (MWRI), Nile Research Institute. (2007–2008). *Unpublished data on Nile River studies* [Unpublished data]. Ministry of Water Resources and Irrigation.

Ministry of Water Resources and Irrigation, General Nile Control Inspection. (1966–1969). *Unpublished reports* [Unpublished reports]. Ministry of Water Resources and Irrigation.

OpenAI. (2025). *Illustrative Figures Generated for Research Purposes Using Artificial Intelligence* [AI-Generated Figures].

U.S. Geological Survey (USGS). (2002). *Landsat TM Satellite Scenes (30 m Resolution)* [Data Set]. United States Geological Survey. https://earthexplorer.usgs.gov

U.S. Geological Survey (USGS). (2023). *Landsat TM Satellite Scenes (30 m resolution)* [Data Set]. United States Geological Survey. https://earthexplorer.usgs.gov

Water Research Center & Nile Research Institute. (1980, 2003, 2007). *Hydro-topographic Maps of the Nile River Bed* (Scale 1:5,000). Water Research Center and Nile Research Institute.

11.2. References

11.2.1. Arabic References

Ahmed, A. O. (2019). *Geomorphology of Erosion and Deposition along the Nile River Banks: Assiut Governorate* (Master's Thesis). Department of Geography, Faculty of Arts, Assiut University.

Aql, M. T. (2003). Erosion and Collapse and their Impact on the Morphology of the Nile Banks between Kom Ombo and Esna: A Morphological Study. *Journal of the Faculty of Arts – Alexandria University*, 26.

Atya, A. (2019). *Morphological Changes in the Nile River channel After the Construction of the High Dam* (Doctoral Dissertation). Department of Geography, Faculty of Arts, Ain Shams University.

Desouki, S. A. (1997). Some Recent Morphological Changes in the Rosetta Branch Channel. *The Arab Geographical Journal*, 29(1).

Desouki, S. A. (2002). Some Recent Geomorphological Changes in the Nile River Channel between Minya and Beni Suef. *The Arab Geographical Journal*, 39(1).

El-Husseiny, E. E. (1988). *The Nile Islands between Nag Hammadi and Assiut – Upper Egypt* (Geographical Messages No. 114). Kuwait Geographical Society & Department of Geography, Kuwait University.

El-Husseiny, E. E. (1991). *The Nile River in Egypt: Its Meanders and Islands – A Geomorphological study*. Cairo University Publishing Center.

El-Khayyat, H. A. S. (2017). *Bank Erosion and Collapse along the Nile River between Esna and Nag Hammadi Barrages – A Geomorphological Study Using GIS and Remote Sensing* (Doctoral dissertation). Department of Geography, Faculty of Arts, Benha University.

Hegab, M. A. (2015). The Water Arms of the Nile River between Sohag and Assiut: A Geomorphological Study. *Journal of the Faculty of Arts, Sohag University*, 38, 50.

Ibrahim, F. A. (1981). *Geomorphology of the*

Damietta Branch (Master's thesis). Department of Geography, Faculty of Arts, Cairo University.

Obaido, I. (1982). *Engineering Geology and Geological Maps* (6th ed.). Monshaat Al-Maaref.

Salama, H. R. (2004). *Foundations of Geomorphology*. Dar Al-Maseera for Publishing and Distribution. Amman, Jordan.

Salama, I. M. M. (2004). *Geomorphological Hazards in the Assiut Region* (Master's Thesis). Department of Geography, Faculty of Arts, Benha University.

Salama, I. M. M. (2006). *A Comparative Study of Geomorphological Hazards along the Damietta and Rosetta Branches* (Doctoral Dissertation). Department of Geography, Faculty of Arts, Benha University.

11.2.2. English References

Ahmed, A. A., Ibrahim, S. A. S., Onyango, O., Fadul, H. M., & Babikir, I. A. (2010). *Nile River Bank Erosion and Protection*.

Baubinienė, A., Satkūnas, J., & Taminskas, J. (2015). Formation of Fluvial Islands and its Determining Factors: Case Study of the River Neris, the Baltic Sea basin. *Geomorphology, 231*, 343–352. https://doi.org/10.1016/j.geomorph.2014.12.043

Bhandari, R. (2019). *River Bank Protection with Gabion Structure: Gabion Mattress*.

Brice, J. C. (1964). *Channel Patterns and Terraces of the Loup Rivers in Nebraska* (U.S. Geological Survey Professional Paper 422-D). United States Government Printing Office.

Craig, R. F. (2004). *Craig's soil mechanics* (7th ed.). Spon Press.

Das, B. M. (2013). *Principles of Geotechnical Engineering* (8th ed.). Cengage Learning.

Dezső, J., Bódis, K., & Szabó, J. (2019). Hydro-Mechanical Behavior of Clay Soils Under Changing Moisture Conditions. *Geomechanics and Engineering, 18*(5), 497–506.

El-Dien, A. A., Takebayashi, H., & Fujita, M. (2014). Stability of River Banks Under Unsteady Flow Conditions. *International Journal of Erosion Control Engineering, 7*(2), 48–55.

Emerson, F. V. (1919). Ferrel's Law and Artillery Firing. *Journal of Geography, 18*(6), 242–242.

Fredlund, D. G., & Rahardjo, H. (1993). *Soil Mechanics for Unsaturated Soils*. John Wiley & Sons.

Gillott, J. E. (1968). *Clay in Engineering Geology*. Elsevier.

Grim, R. E. (1968). *Clay Mineralogy* (2nd ed.). McGraw-Hill.

Holtz, R. D., Kovacs, W. D., & Sheahan, T. C. (2011). *An Introduction to Geotechnical Engineering* (2nd ed.). Pearson Education.

Koerner, R. M. (2012). *Designing with Geosynthetics – Vol. 1* (Vol. 1). Xlibris Corporation.

Lambe, T. W., & Whitman, R. V. (1969). *Soil Mechanics*. John Wiley & Sons.

Lane, P. A., & Griffiths, D. V. (2000). Assessment of Stability of Slopes under Drawdown Conditions. *Journal of Geotechnical and Geoenvironmental Engineering, 126*(5), 443–450. https://doi.org/10.1061/(ASCE)1090-0241(2000)126:5(443)

Leopold, L. B., & Langbein, W. B. (1966). *River Meanders: Theory of Minimum Variance* (U.S. Geological Survey Professional Paper 422-H). U.S. Government Printing Office.

Lu, N., & Likos, W. J. (2004). *Unsaturated Soil Mechanics*. John Wiley & Sons.

McTainsh, G. H. (1971). Stream bank erosion, Banks Peninsula, New Zealand (Unpublished master's thesis). University of Canterbury, Christchurch, New Zealand.

Mitchell, J. K., & Soga, K. (2005). *Fundamentals of Soil Behavior*.

Moore, D. M., & Reynolds, R. C. (1997). *X-Ray Diffraction and the Identification and Analysis of Clay Minerals* (2nd ed.). Oxford University Press.

Murray, R. S. (2007). Soils and Soil Physical Properties. In *Soil Science: An Introduction*. University of Sydney.

Prasad, S. K., Indulekha, K. P., & Balan, K. (2016). Analysis of Groyne Placement on Minimising River Bank Erosion. *Procedia*

Technology, 24, 47–53.

Rady, M. A. (1976). *River Bed Degradation below Large Capacity Dams and its Application for the Nile after High Aswan Dam Construction* (Doctoral Dissertation, Technical University of Szczecin, Poland).

Rahardjo, H., Satyanaga, A., & Leong, E. C. (2007). Controlled-Suction Tests for Unsaturated Residual Soils. *Geotechnical Testing Journal, 30*(1), 1–8.

Roy, A. G., Roy, R., & Bergeron, N. (1988). Hydraulic Geometry and Changes in Flow Velocity at a River Confluence with Coarse Bed Material. *Earth Surface Processes and Landforms, 13*(7), 583–598. https://doi.org/10.1002/esp.3290130704

Saber, A. I. M. (2023). Recent trends in the geomorphology of rivers and criteria for the degrees of their danger. *Journal of Sustainable Development in Social and Environmental Sciences*, *2*(2), 59-68. https://doi.org/10.21608/jsdses.2023.201252.1015

Saber, A. I. M., & Hassan, H. T. A. (2024). The impact of spur dikes on the dynamics of erosion and deposition processes in the Nile River in Abnub Area: A study in engineering geomorphology using artificial intelligence. *Journal of the Faculty of Arts Port Said University*, *27*(27), 172-223. https://doi.org/10.21608/jfpsu.2023.242175.1308

Saber, A. I. M., & Hassan, H. T. A. (2025). Spatial modelling of the impact of bridges on the geomorpho-terrain characteristics of the Nile streambed and their hazards in El-Zamalik Area, Egypt: A Study in engineering geomorphology using geomatics techniques. *Journal of Sustainable Development in Social and Environmental Sciences*, *4*(1), 103-164. https://doi.org/10.21608/jsdses.2025.370221.1045

Sadek, K. A. N. (2010). Inundations by High Releases Downstream High Aswan Dam. *Nile Basin Water Science & Engineering Journal, 3*(2).

Sadek, N., & Hekal, N. (2008). Prediction of the Future Situation of the River Nile Navigational Path. In *Twelfth International Water Technology Conference (IWTC12 2008)*, Alexandria, Egypt (pp. 323–336).

Schuster, R. L., & Wieczorek, G. F. (2018). Landslide triggers and types. In *Landslides* (pp. 59-78). Routledge.

Strahler, A. N. (1964). Quantitative geomorphology of drainage basins and channel networks. In V. T. Chow (Ed.), *Handbook of applied hydrology* (pp. 39–76). McGraw-Hill.

Yao, J., Li, Y., Zhang, D., Zhang, Q., & Tao, J. (2019). Wind effects on hydrodynamics and implications for ecology in a hydraulically dominated river-lake floodplain system: Poyang Lake. *Journal of Hydrology, 571*, 103–113. https://doi.org/10.1016/j.jhydrol.2019.01.057